Dynamical effects on photoluminescence spectra from first principles: A many-body Green's function approach

Pierluigi Cudazzo
Dipartimento di Fisica, Universitá di Trento, via Sommarive 14, I-38123 Povo, Italy and European Theoretical Spectroscopy Facility (ETSF)

(Received 11 May 2023; revised 14 September 2023; accepted 15 September 2023; published 2 October 2023)

Coupling of excitations, arising from electronic correlation or electron-phonon interaction, leads to intriguing effects on the spectra of materials. Current approximations to calculate photoluminescence spectra most often describe this coupling insufficiently. Starting from basic equations of many-body perturbation theory, we derive a cumulant formulation for photoluminescence spectra that contains excitonic effects and the coupling between excitons and other degrees of freedom such as plasmons and phonons. The cumulant approach allows us to include dynamical effects arising from the electronic correlation and electron-phonon coupling in a simple and intuitive way. It can be implemented as a postprocessing of state-of-the-art out-of-equilibrium Bethe-Salpeter calculations of excitonic states.

DOI: 10.1103/PhysRevB.108.165101

I. INTRODUCTION

Photoluminescence (PL) spectroscopy is a widely-used technique for characterization of the optical and electronic properties of semiconductors and molecules. The technique itself is fast, contactless, and nondestructive. Moreover it requires minimal sample preparation and allows pinpointing very small features (micron scale) on ultrathin samples ($<$1 nm). This makes PL one of the most used techniques for the study of two-dimensional systems. Despite all this, a full *ab initio* method that allows for prediction of PL spectra in real materials is still missing.

In the last two decades, the method of Green's functions, namely many-body perturbation theory (MBPT) [1–3], has been successfully applied to the study of the optical properties of semiconductors. It provides an accurate *ab initio* description of both electronic band structures as well as excitonic effects that in this framework are addressed through the solution of the Bethe-Salpeter equation (BSE) [2,3] for the electronic polarizability. A rigorous formulation for the luminescence signal in terms of Green's functions has been derived by Hannewald and coworkers [4]. Here the spontaneous emission is obtained by explicitly solving the BSE on the Keldysh contour [5]. This approach treats absorption and luminescence on equal footing and allows one to calculate the luminescence spectrum for arbitrary nonthermal distributions. As a consequence, when combined with modern methods for the description of photoexcited carriers relaxation [6], it gives access also to out-of-equilibrium spectroscopies such as transient absorption and time resolved PL [7,8].

However, although the BSE is formally exact, in state-of-the-art calculations it is solved in the static approximation; i.e., taking the first-order expansion of the BSE kernel in terms of the statically screened Coulomb interaction [3,9]. In this way all dynamical effects associated to the dynamical fluctuations of the electronic charge and the lattice are completely neglected. As a matter of fact, dynamical effects are directly related to the explicit frequency dependence of the effective interaction between particles and are responsible for shifts and broadening of peaks, as well as additional structures called satellites [9]. The latter are pure many-body effects induced by electronic correlation and electron-phonon interaction and often dominate the low energy region of the PL spectra of real materials. An example is represented by the plasmon satellites observed in the PL spectra of doped 2D transition metal dichalcogenides [10], or in excitonic systems coupled with metallic nanoparticles used in plasmonic architectures [11] or phonon satellites that play a key role in the PL spectra of polar semiconductors [12], molecular crystals [13], quantum dots [14], and indirect-gap semiconductors [15–17].

The fully dynamical BSE is extremely complicated to solve [18,19], and its solution might not be worth the effort. Indeed, the BSE with a first-order kernel is similar to the Dyson equation for the one-particle Green's function with the self-energy evaluated at the first order in the screened Coulomb (or electron-phonon) interaction that often fails for satellites [9]. Rather than a scheme based on a Dyson equation, a cumulant approach for the two-particle polarizability [20,21] reflecting a picture of coupled bosons, appears more promising. It is the exact solution for a two-level limiting case [22], and it is additionally motivated by the success of an increasing number of *ab initio* calculations for the one-particle Green's function for the description of both plasmonic [22–24] and phononic [25,26] satellites in the photoemission spectra.

In this article, starting from the recently developed cumulant expansion for the electronic polarizability [20], we generalize this approach to the out-of-equilibrium conditions (i.e., in presence of photoexcited carriers). This will allow including dynamical effects beyond state-of-the-art BSE in a systematic way, treating the electronic correlation and electron-phonon interaction on the same footing. In particular, following Refs. [20,21], the derivation is done in two main

steps. First of all, starting from the fully dynamical BSE on the Keldysh contour we obtain a Dyson-like equation for the two-time electronic polarizability that represents the exciton propagator and provides the spectrum of neutral excitations. This requires the introduction of an exciton self-energy related to the dynamically screened Coulomb potential and the electron-phonon interaction. At this point, the cumulant expression for the exciton propagator comes out naturally. Indeed, in analogy with the one-particle Green's function, the cumulant coefficient is obtained imposing that the first-order expansion of a cumulant ansatz for the exciton propagator matches the first-order expansion of the Dyson equation.

The paper is organized as follows: In Sec. II we present a short overview of the basic theory of PL highlighting the relation between spectroscopic quantities and correlation functions while in Sec. III, starting from the perturbation expansion of the polarizability we derive an approximation for the exciton self-energy. This will allow a partial resummation of the perturbation series using a Dyson-like equation as well as a cumulant expansion. In Sec. IV we derive the the explicit expression of the cumulant coefficient in the case of exciton-phonon coupling and in Sec. V the approach will be applied to a simple model system as an illustrative example. The last section is devoted to the conclusions.

II. PHOTOLUMINESCENCE SPECTRA IN THE FRAMEWORK OF MBPT

A rigorous formulation for the luminescence signal in terms of the Green's functions has been derived by Hannewald *et al.* [4]. It follows the theory on measurement of fluctuating quantities by Butcher and Ogg [27], where the field amplitudes are passed through a spectral filter and the intensity after the filter is measured during a time interval of length T, in the limit $T \to \infty$. As result, the measured signal is proportional to the autocorrelation function of the field amplitudes, which is directly related to the transverse current density fluctuations [28],

$$p(\omega) = \frac{\omega^2}{4\pi^2}\frac{1}{\Omega}\int d\mathbf{r}\int d\mathbf{r}'\int_{-\infty}^{+\infty} dt\, e^{i\omega(t-t')} \times \left\langle \Delta\hat{\mathbf{j}}^T(\mathbf{r},t)\cdot\Delta\hat{\mathbf{j}}^T(\mathbf{r}',t')\right\rangle, \quad (1)$$

where we used atomic units and the superscript T refers to the transverse current density. The transverse current density fluctuations are directly related to the lesser component of the density correlation function $\mathcal{L}^<(\mathbf{r}t,\mathbf{r}'t')$ that in the framework of MBPT is obtained from the evaluation of the two-particle four-point correlation function through the relation $\mathcal{L}^<(\mathbf{r}t,\mathbf{r}'t') = -iL(\mathbf{r}t,\mathbf{r}'t',\mathbf{r}t,\mathbf{r}'t')$. For instance, for an isotropic medium (as in the case of cubic semiconductors), the transverse current density correlation function for a given polarization (α) can be written as

$$\int d\mathbf{r}\int d\mathbf{r}'\left\langle \Delta\hat{j}^T_\alpha(\mathbf{r},t)\cdot\Delta\hat{j}^T_\alpha(\mathbf{r}',t')\right\rangle = \sum_{\mathbf{vcv'c'}}\langle\phi_\mathbf{c}|\hat{p}_\alpha|\phi_\mathbf{v}\rangle\langle\phi_\mathbf{v'}|\hat{p}_\alpha|\phi_\mathbf{c'}\rangle i\mathcal{L}^{\mathbf{cv}<}_{\mathbf{c'v'}}(t,t'), \quad (2)$$

where $\hat{p}_\alpha$ are dipoles operators and we expanded $\mathcal{L}$ in the basis of Bloch states (see Appendix A for the definition of the matrix elements) with indexes $\mathbf{c}$ and $\mathbf{v}$ running over the conduction and valence bands, respectively. In addition we use the compact notation $\mathbf{i} = (i,\mathbf{k}_i)$ to indicate, for a given Bloch state, the band index i and the corresponding wave vector $\mathbf{k}_i$. Since in Eq. (2) we take the optical limit, the conservation of Bloch wave vector requires that $\mathbf{k}_c = \mathbf{k}_v$ and $\mathbf{k}'_c = \mathbf{k}'_v$.

Finally, following Ref. [4], Eq. (1) can be further simplified by treating nonresonant transitions associated to crystal local field effects via a static screening. In other words, we approximate the density correlation function by $\mathcal{L} \approx \mathcal{P}/\epsilon$, where the polarizability $\mathcal{P}$ is the irreducible part of $\mathcal{L}$ and ϵ is the static dielectric constant. Under these conditions, Eq. (1) becomes

$$p(\omega) = \frac{2\omega^2}{4\pi^2\epsilon}\frac{i}{\Omega}\sum_{\alpha\mathbf{vcv'c'}}\langle\phi_\mathbf{c}|\hat{p}_\alpha|\phi_\mathbf{v}\rangle\langle\phi_\mathbf{v'}|\hat{p}_\alpha|\phi_\mathbf{c'}\rangle\mathcal{P}^{\mathbf{cv}<}_{\mathbf{c'v'}}(\omega') \quad (3)$$

where the factor 2 arises from the sum over the spin variable. Thus the evaluation of the photoluminescence spectrum reduces to the evaluation of the polarizability $\mathcal{P}(t,t')$, which is directly linked to the four-point polarizability [i.e., $\mathcal{P}(t,t') = -iP(t,t',t,t')$] and can be treated in the framework of MBPT.

III. DYSON EQUATION FOR THE EXCITON PROPAGATOR ON THE KELDYSH CONTOUR

In the framework of MBPT the four-point polarizability P is formally obtained from the solution of the BSE [2,3] that, expanded on a generic basis set, becomes a matrix equation of the form

$$\hat{P}(z_{1423}) = \hat{P}_0(z_{1423}) + \hat{P}_0(z_{1\bar{4}\bar{2}\bar{1}})\hat{\Xi}(z_{\bar{1}\bar{4}\bar{2}\bar{3}})\hat{P}(z_{\bar{3}\bar{4}\bar{2}\bar{3}}). \quad (4)$$

Here z_i are time variables on the Keldysh contour and repeated indices are integrated over. Moreover, $\hat{P}_0(z_{1\bar{4}\bar{2}\bar{1}}) = \hat{G}(z_{1\bar{1}})\hat{G}(z_{\bar{4}\bar{2}})$ is the operator associated to the uncorrelated four-point polarizability ($\hat{G}$ denoting the full interacting one particle propagator) and $\hat{\Xi}$ is the kernel that can be obtained from a perturbative expansion in terms of the effective particle-particle interaction $\hat{W}^{\text{tot}}$. The latter is the sum of the dynamically screened Coulomb interaction (W^C) and the Coulomb interaction screened by lattice vibrations (W^{ph}) [29,30].

In state-of-the-art calculations, $\hat{G}$ is evaluated taking the COHSEX [31] or quasiparticle GW^C approximation [32] for the electron self-energy (eventually including the electron-phonon coupling in the Allen-Cardona scheme [33,34]) and $\hat{\Xi}$ is evaluated at the first order in the statically screened Coulomb interaction. In this way dynamical effects induced by the electronic correlation and the electron-phonon coupling are completely neglected.

In the following we will refer to this approximation for Eq. (4) as static Bethe-Salpeter equation (SBSE). In this case, since $\hat{\Xi}$ is time independent, the SBSE can be written as a Dyson like equation for the two-time polarizability $\hat{\mathcal{P}}(z_{13}) = -i\hat{P}(z_{1313})$. In addition, under quasistationary conditions all the components of the Keldysh functions involved in Eq. (4) depend only on the time differences [4]. This allows solving the SBSE in frequency space in analogy with what one does under equilibrium conditions [4,35].

In the case of the full dynamical BSE, instead, because of the explicit time dependence of the kernel, Eq. (4) cannot

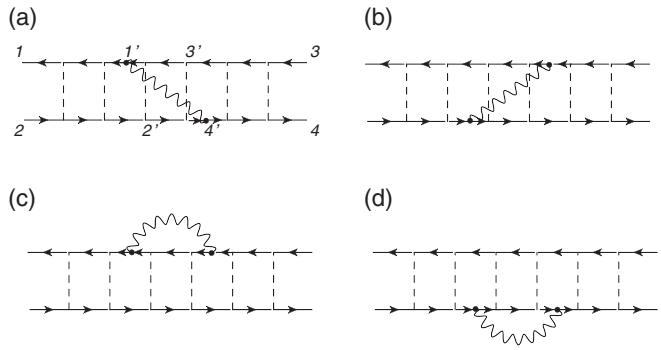

FIG. 1. Feynman diagrams associated to the first-order expansion P in terms of W. Diagrams (a)–(d) correspond to the lines one to four in Eq. (8). Arrows are the one-particle Green's function $\bar{G}$, dashed lines denote W_0^C, and wiggly lines correspond to W.

be rewritten in terms of a two-time propagator only and it is hardly solvable even considering the simplest first-order expansion for $\hat{\Xi}$ in terms of $\hat{W}^{\rm tot}$ [18,19]. Nevertheless, the quantity we are interested into is $\hat{\mathcal{P}}$ and not $\hat{P}$. This suggests that it is more convenient looking for an approximate Dyson like equation for $\hat{\mathcal{P}}$ with the following structure:

$$\hat{\mathcal{P}}(z_{13}) = \hat{\bar{\mathcal{P}}}(z_{13}) + \hat{\bar{\mathcal{P}}}(z_{11'})\hat{\Pi}(z_{13'})\hat{\mathcal{P}}(z_{3'3}) \tag{5}$$

without passing through the evaluation of the four time $\hat{P}$. The operator $\hat{\bar{\mathcal{P}}}$ in Eq. (5) represents the two-time polarizability obtained from the solution of the SBSE and plays the role of a noninteracting exciton propagator. The operator $\hat{\Pi}$, on the other hand, takes the physical meaning of an effective exciton self-energy describing all dynamical effects beyond the SBSE induced by the electronic correlation and the coupling with lattice vibrations. This equation provides a formally exact representation for $\hat{\mathcal{P}}$ by virtue of the basic theorems of time-dependent density functional theory [36,37] and constitutes the starting point for the cumulant expansion.

In order to find an approximation for $\hat{\Pi}$, we start with the known perturbation expansion of $\hat{P}$ in terms of $\hat{W}^{\rm tot}$ and the Hartree Green's function [38]. Then, following Ref. [20], we split the dynamically screened Coulomb interaction in a static contribution $\hat{W}_s^C(z_{12}) = \hat{W}^C(\omega = 0)\delta(z_1 - z_2)$ and a dynamical part ($\Delta\hat{W}^C$), $\hat{W}^C(z_{12}) = \hat{W}_s^C(z_{12}) + \Delta\hat{W}^C(z_{12})$. This also means that we can write the effective particle-particle interaction as $\hat{W}^{\rm tot}(z_{12}) = \hat{W}_s^C(z_{12}) + \hat{W}(z_{12})$, with the full dynamical part of the interaction given by the following expression:

$$\hat{W}(z_{12}) = \Delta\hat{W}^C(z_{12}) + \hat{W}^{\rm ph}(z_{12}). \tag{6}$$

In particular, when $\hat{W}$ is set to zero in the full perturbation expansion of $\hat{P}$ and $\hat{W}_s^C$ is treated in the Tamm-Dancoff approximation (TDA) [39,40], we recover the SBSE with the one particle Green's function evaluated in COHSEX approximation and the static kernel $\hat{\Xi}_s = i\hat{W}_s^C$ [20]. To overcome the static approximation, we consider corrections to first order in $\hat{W}$, i.e., we linearize the full perturbation expansion of $\hat{P}$ respect to $\hat{W}$ treating W_s^C in TDA. This leads to the series of Feynman diagrams in Fig. 1 evaluated at all orders in $\hat{W}_s^C$. The corresponding expression for $\hat{\mathcal{P}}$ is given by the following equation [20,21]:

$$\hat{\mathcal{P}}(z_{13}) = \hat{\bar{\mathcal{P}}}(z_{13}) - i\hat{\bar{P}}(z_{12'11'})\hat{\mathcal{K}}(z_{1'4'2'3'})\hat{\bar{P}}(z_{3'34'3}), \tag{7}$$

where the full dynamical kernel $\hat{\mathcal{K}}$ can be directly read from Fig. 1 [21],

$$\begin{aligned}\hat{\mathcal{K}}(z_{1423}) = {} & i\hat{W}(z_{14})\hat{\bar{P}}(z_{14\bar{2}\bar{3}})\hat{\bar{G}}^{-1}(z_{\bar{3}\bar{3}})\hat{\bar{G}}^{-1}(z_{\bar{2}\bar{2}}) \\ & + i\hat{W}(z_{32})\hat{\bar{P}}(z_{\bar{1}4\bar{2}3})\hat{\bar{G}}^{-1}(z_{1\bar{1}})\hat{\bar{G}}^{-1}(z_{2\bar{2}}) \\ & + i\hat{W}(z_{13})\hat{\bar{P}}(z_{1\bar{4}\bar{2}3})\hat{\bar{G}}^{-1}(z_{\bar{2}\bar{2}})\hat{\bar{G}}^{-1}(z_{4\bar{4}}) \\ & + i\hat{W}(z_{42})\hat{\bar{P}}(z_{\bar{1}4\bar{2}3})\hat{\bar{G}}^{-1}(z_{\bar{3}\bar{3}})\hat{\bar{G}}^{-1}(z_{1\bar{1}}).\end{aligned} \tag{8}$$

Here $\hat{\bar{P}}$ denotes the four-time polarizability obtained from the solution of the SBSE and $\hat{\bar{G}}$ the COHSEX one-particle Green's function. An equivalent expression for $\hat{\mathcal{K}}$ can be obtained taking the functional derivative respect to G of a $GW\Gamma$ one-electron self-energy, where W is assumed to be independent from G and the vertex Γ is evaluated in the static ladder approximation [41].

The diagrammatic representation of P in Fig. 1 illustrates that we include the complete series of ladder diagrams in the static effective Coulomb interaction $\hat{W}_s^C$ responsible for excitonic effects, whereas dynamical effects are included through an effective kernel evaluated at the first order in $\hat{W}$. The comparison between first-order W expansion of Eqs. (7) and (5) leads the formal expression for first-order $\hat{\Pi}$,

$$\hat{\Pi}(z_{13}) = -i\hat{\bar{\mathcal{P}}}^{-1}(z_{1\bar{1}})\hat{\bar{P}}(z_{\bar{1}2'\bar{1}1'})\hat{\mathcal{K}}(z_{1'4'2'3'})\hat{\bar{P}}(z_{3'\bar{3}4'\bar{3}})\hat{\bar{\mathcal{P}}}^{-1}(z_{\bar{3}\bar{3}}). \tag{9}$$

The basic issue in Eq. (9) is the evaluation of the convolution $\hat{\bar{P}}\hat{\mathcal{K}}\hat{\bar{P}}(z_{\bar{1}\bar{2}})$ on the Keldysh contour that can be traced back to the two prototypical Feynman diagrams shown in the left side of Figs. 2(a) and 2(b) evaluated at all orders in $\hat{W}_s^C$. However, expanding on the basis of Bloch states and using the generalized Langreth rules for multi-argument Keldysh functions [42], we can derive the following identity:

$$\begin{aligned} iR_{\mathbf{nm}} & \int_\gamma dz_{1'}\bar{G}_{\mathbf{n}}(z_{11'})\bar{G}_{\mathbf{n}'}(z_{1'2'})\bar{G}_{\mathbf{m}}(z_{2'1})W(z_{3'1'}) \\ & = \int_\gamma dz_{1'}\bar{G}_{\mathbf{n}}(z_{13'})\bar{G}_{\mathbf{n}'}(z_{3'2'})\bar{G}_{\mathbf{m}}(z_{3'1})\bar{G}_{\mathbf{m}}(z_{2'3})W(z_{3'1'}) \\ & \quad - \int_\gamma dz_{1'}\bar{G}_{\mathbf{n}}(z_{12'})\bar{G}_{\mathbf{n}}(z_{2'3'})\bar{G}_{\mathbf{n}'}(z_{3'2'})\bar{G}_{\mathbf{m}}(z_{21})W(z_{3'1'}).\end{aligned} \tag{10}$$

Here $\mathbf{n} = (n, \mathbf{k}_n)$ denote quasiparticle Bloch states in which $\hat{\bar{G}}$ is diagonal and $R_{\mathbf{nm}} = f_{\mathbf{m}} - f_{\mathbf{n}}$ are Pauli blocking factors ($f_{\mathbf{n}}$ being electron occupation number of state $\mathbf{n}$). Equation (10) allows inserting in each interaction vertex (black dots in Fig. 2) additional space-spin points that are integrated over (red dots in Fig. 2). Moreover, their time coordinates on the Keldysh contour is chosen equal to an already existing time integration point. In this way each Feynman diagram splits into four contributions that can be rearranged in the convolution $\hat{\mathcal{P}}_0\hat{\mathcal{F}}\hat{\mathcal{P}}_0(z_{13})$, $\mathcal{F}$ being a two-time Keldysh function and $\hat{\mathcal{P}}_0$ the

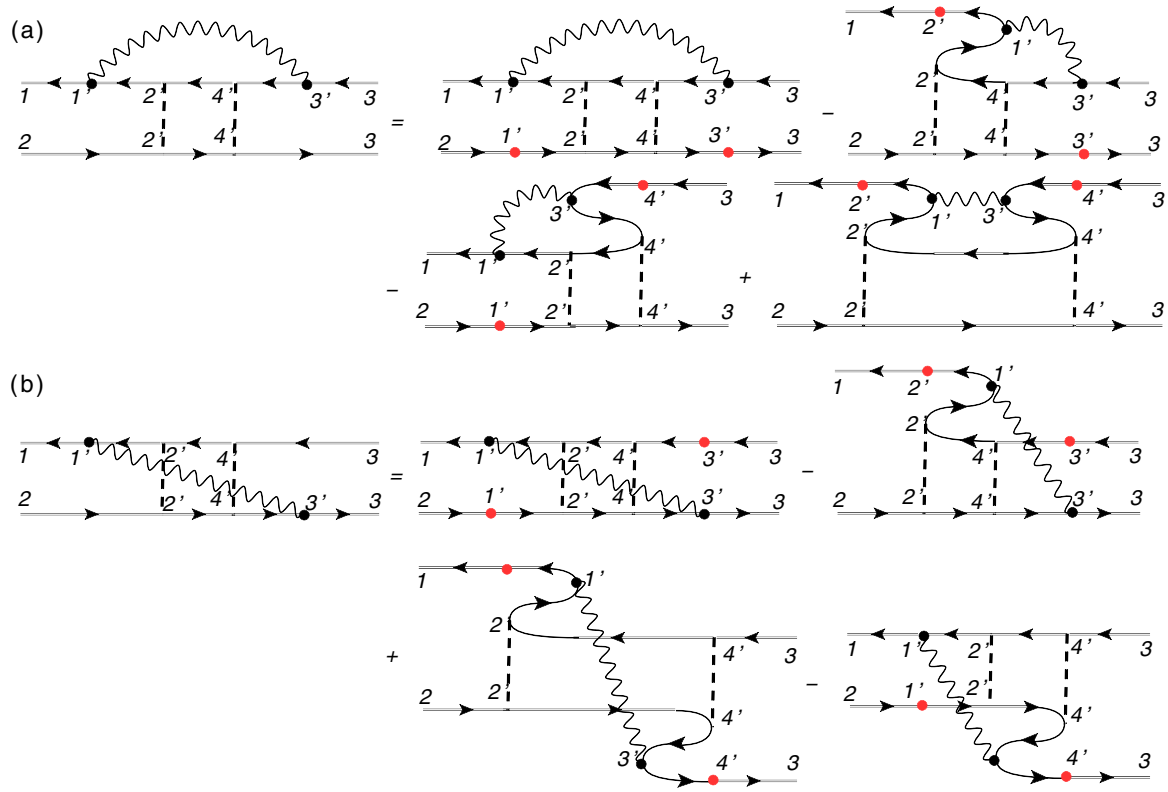

FIG. 2. [(a), (b)] Prototypical first-order diagrams in W. Here arrows represent $\bar{G}$, the dashed line the SBSE kernel W_s^C, and the wiggly lines stand for W. Red indicates inserts needed to express the result in terms of the two-times $\bar{\mathcal{P}}$ and $\mathcal{P}_0$ (see text).

two-time uncorrelated polarizability. This leads the identity

$$\hat{\bar{P}}(z_{\bar{1}2'\bar{1}1'})\hat{\mathcal{K}}(z_{1'4'2'3'})\hat{\bar{P}}(z_{3'\bar{3}4'\bar{3}}) = \hat{\bar{\mathcal{P}}}(z_{\bar{1}1'})\hat{\mathcal{F}}(z_{1'3'})\hat{\bar{\mathcal{P}}}(z_{3'\bar{3}}) \quad (11)$$

that inserted in Eq. (9) allows to identify the exciton self-energy with $\mathcal{F}$, $\hat{\Pi}(z_{13}) = -i\hat{\mathcal{F}}(z_{13})$.

The complete expression of $\hat{\Pi}$ is reported in Appendix A. Here we consider its expression in the limit of small density of photo-excited carriers that as discussed in Appendix A, is the sum of a static (${}^s\Pi$) and a full dynamical (${}^d\Pi$) contribution,

$$\begin{aligned} {}^s\Pi^{\mathbf{cv}}_{\mathbf{c'v'}}(z_{13}) = -\frac{1}{R_{\mathbf{cv}}}\Big\{ &\frac{1}{2}\delta_{\mathbf{vv'}}\delta(z_{13})\big[W^{\mathbf{cc'}}_{\bar{\mathbf{v}}\bar{\mathbf{v}}}\cdot i\mathcal{P}_0^{\mathbf{c}\bar{\mathbf{v}}}\big](z_{31}) + \frac{1}{2}\delta_{\mathbf{vv'}}\delta(z_{13})\big[i\mathcal{P}_0^{\mathbf{c'}\bar{\mathbf{v}}}\cdot W^{\mathbf{cc'}}_{\bar{\mathbf{v}}\bar{\mathbf{v}}}\big](z_{31}) + \frac{1}{2}\delta_{\mathbf{cc'}}\delta(z_{13})\big[W^{\bar{\mathbf{c}}\bar{\mathbf{c}}}_{\mathbf{v'v}}\cdot i\mathcal{P}_0^{\bar{\mathbf{c}}\mathbf{v}}\big](z_{31}) \\ &+\frac{1}{2}\delta_{\mathbf{cc'}}\delta(z_{13})\big[i\mathcal{P}_0^{\bar{\mathbf{c}}\mathbf{v'}}\cdot W^{\bar{\mathbf{c}}\bar{\mathbf{c}}}_{\mathbf{v'v}}\big](z_{31})\Big\}\frac{1}{R_{\mathbf{c'v'}}}, \end{aligned} \quad (12)$$

$${}^d\Pi^{\mathbf{cv}}_{\mathbf{c'v'}}(z_{13}) = \frac{1}{R_{\mathbf{cv}}}\big\{i\bar{\mathcal{P}}^{\mathbf{c}_1\mathbf{v}}_{\mathbf{c}_2\mathbf{v'}}(z_{13})W^{\mathbf{cc'}}_{\mathbf{c}_2\mathbf{c}_1}(z_{31}) + i\bar{\mathcal{P}}^{\mathbf{cv}_1}_{\mathbf{c'v}_2}(z_{13})W^{\mathbf{v}_1\mathbf{v}_2}_{\mathbf{v'v}}(z_{31}) - i\bar{\mathcal{P}}^{\bar{\mathbf{c}}\mathbf{v}}_{\mathbf{c'}\bar{\mathbf{v}}}(z_{13})W^{\mathbf{c}\bar{\mathbf{v}}}_{\mathbf{v'}\bar{\mathbf{c}}}(z_{31}) - i\bar{\mathcal{P}}^{\mathbf{c}\bar{\mathbf{v}}}_{\bar{\mathbf{c}}\mathbf{v'}}(z_{13})W^{\bar{\mathbf{v}}\mathbf{c'}}_{\bar{\mathbf{c}}\mathbf{v}}(z_{31})\big\}\frac{1}{R_{\mathbf{c'v'}}}, \quad (13)$$

where we use the usual convention that repeated indexes are summed up. In the following, since ${}^s\Pi$ causes only a shift of the exciton energy and does not have any effect on the exciton lifetime and satellites, we will safely take $\Pi(z_{13}) =^d \Pi(z_{13})$ and include ${}^s\Pi$ in the definition of the exciton energy.

Once an approximate expression for the exciton self-energy is found, the inclusion of the dynamical effects beyond the SBSE reduces to the solution of Eq. (5). A natural way to address this problem is expanding Eq. (5) on the basis of excitonic states. However, in this case, in contrast with the standard Dyson equation for one particle Green's function, the noninteracting propagator $\hat{\bar{\mathcal{P}}}$ is not diagonal. This is a consequence of the Pauli blocking factor arising from the presence of photo-excited carriers [16,35]. In order to avoid all the complications arising from the presence of the off-diagonal components of the exciton propagator, it is convenient working with the symmetrized propagator $\hat{\mathcal{B}}$ instead of $\hat{\mathcal{P}}$ that in the static limit, as discussed in Appendix B, is diagonal in the basis of the eigenstates of the symmetrized excitonic Hamiltonian [43]. In the basis of Bloch states it is defined in such a way that $\mathcal{P}^{\mathbf{cv}}_{\mathbf{c'v'}}(z_{13}) = \sqrt{R_{\mathbf{cv}}}\mathcal{B}^{\mathbf{cv}}_{\mathbf{c'v'}}(z_{13})\sqrt{R_{\mathbf{c'v'}}}$ and similarly for $\bar{\mathcal{B}}^{\mathbf{cv}}_{\mathbf{c'v'}}$ and $\bar{\mathcal{P}}^{\mathbf{cv}}_{\mathbf{c'v'}}$. Thus, when we move in the basis of the symmetrized excitonic states, $\hat{\mathcal{B}}$ satisfy the following equation:

$$\mathcal{B}_{\lambda\lambda'}(z_{13}) = \bar{\mathcal{B}}_{\lambda}(z_{13})\delta_{\lambda\lambda'} + \bar{\mathcal{B}}_{\lambda}(z_{11'})\tilde{\Pi}_{\lambda\alpha}(z_{1'3'})\mathcal{B}_{\alpha\lambda'}(z_{3'3}), \quad (14)$$

where the Greek indexes label the eigenstates of the symmetrized excitonic Hamiltonian and $\tilde{\Pi}^{cv}_{c'v'} = \sqrt{R_{cv}}\Pi^{cv}_{c'v'}\sqrt{R_{c'v'}}$. In particular, in the basis of symmetrized excitonic states $\tilde{\Pi}$ can be written in a more compact way and takes the structure of the GW self-energy for one-particle excitations with G and W replaced by $\bar{\mathcal{B}}$ and $\mathcal{W}$, respectively (see Appendix B),

$$\tilde{\Pi}_{\lambda\lambda'}(z_{13}) = i\bar{\mathcal{B}}_{\alpha}(z_{13})\mathcal{W}_{\lambda\alpha\alpha\lambda'}(z_{31}). \tag{15}$$

The effective exciton-exciton interaction $\mathcal{W}$ is given by matrix elements of W appropriately weighted with the Pauli blocking factor that can be read from Fig. 2 and that are detailed in Appendix B. Equation (15) reflects a picture of an exciton coupled with other bosonic-like excitations associated to the poles of W. In principle they include phonons and, depending from the degree of approximation used to evaluate ΔW^C, plasmons and other excitons.

Equation (15) is the generalization to the out-of-equilibrium conditions of the exciton self-energy introduced in Refs. [20,21] and represents the main result of this section. On one side, it allows including dynamical effects through Eq. (14), on the other side it is the key quantity for the partial resummation of higher-order terms through the cumulant expansion.

It is important to note that a Dyson-like equation with the same structure of the exciton self-energy can be formally written for $\hat{\mathcal{L}}$ as well. To this end it is enough to use $\hat{\Xi}_s = -2i\hat{v} + i\hat{W}^C_s$ for the kernel of the SBSE with $\hat{v}$ denoting the operator associated to the bare Coulomb potential entering as an exchange electron-hole interaction. In this way the SBSE will lead to $\hat{\tilde{L}}$ instead of $\hat{\tilde{P}}$. Repeating step by step the previous procedure we can derive a Dyson-like equation equivalent to Eq. (14) for the symmetrized exciton propagator associated to $\hat{\mathcal{L}}$. This would allow for an explicit treatment of crystal local fields in Eq. (3). Nevertheless, here for simplicity, we prefer to work with $\hat{\mathcal{P}}$ and approximate crystal local field effects renormalizing the spectrum with the dielectric constant in accordance with Ref. [4].

IV. EXCITON-PHONON COUPLING AND PHONON ASSISTED PHOTOLUMINESCENCE

A. Exciton-phonon self-energy

In the remaining part of the article we will focus on the effect of the electron-phonon coupling treating electronic correlations in a quasistatic approximation. To this end, we include the contribution of ΔW^C in the single-particle self-energy that is evaluated in standard GW^C instead of COHSEX approximation. As a consequence, according with the perturbative GW^C scheme [44,45], $\bar{G}$ is the Kohn-Sham Green's function with Kohn-Sham energy shifted by the quasiparticle corrections evaluated in G_0W_0 approximation. Moreover, we take $W = W^{\rm ph}$ with the phonon frequencies and the electron-phonon matrix elements evaluated in the framework of density functional perturbation theory (DFPT) [46]. This is consistent with our treatment of W^C and $\bar{G}$ [47]. We emphasize that, being the formulation of this approach completely general and independent from the approximations used to treat lattice vibrations, it allows to take into account corrections beyond standard DFPT as well. They include, for example, dynamical screening in the evaluation of the electron-phonon matrix elements [48] or nonadiabatic effects in the evaluation of the phonon frequencies [49]. In addition, here we take the assumption that nuclei are fixed at their ground-state positions even if, in principle upon excitation, they could move modifying the emission spectra (Stokes shift). This effect could be taken into account combining our approach with the recently developed constrained DFT scheme for the evaluation of the atomic positions in the excited state [50].

Writing $W^{\rm ph}$ in terms of the phonon propagator and electron-phonon matrix elements [30], the diagonal part of the exciton self-energy can be written as

$$\tilde{\Pi}_{\lambda\mathbf{q}}(z_{13}) = \frac{i}{N}\sum_{\alpha\mu\bar{\mathbf{q}}} \left|g^{\rm exc}_{\alpha\lambda;\mu}(\mathbf{q}\bar{\mathbf{q}})\right|^2 \bar{\mathcal{B}}_{\alpha\mathbf{q}+\bar{\mathbf{q}}}(z_{13})D_{\mu\bar{\mathbf{q}}}(z_{31}), \tag{16}$$

where D denotes the phonon propagator, $g^{\rm exc}$ the exciton-phonon matrix elements as detailed in Appendix C, and $\alpha(\lambda)$ and μ the exciton and phonon band indexes, respectively. In principle, in the case of the exciton-phonon interaction, we should consider also the Debye-Waller contribution to the exciton self-energy [51]. However, this term is static and can be included in the definition of the exciton energy.

Under quasistationary conditions and under the assumption that the self-energy is diagonal in the basis of excitonic states, Eq. (14) reduces to the following set of coupled equations that can be solved in the frequency space,

$$\mathcal{B}^{\lessgtr}_{\lambda\mathbf{q}}(\omega) = \mathcal{B}^{R}_{\lambda\mathbf{q}}(\omega)\tilde{\Pi}^{\lessgtr}_{\lambda\mathbf{q}}(\omega)\mathcal{B}^{A}_{\lambda\mathbf{q}}(\omega), \tag{17}$$

$$\mathcal{B}^{R/A}_{\lambda\mathbf{q}}(\omega) = \bar{\mathcal{B}}^{R/A}_{\lambda\mathbf{q}}(\omega) + \mathcal{B}^{R/A}_{\lambda\mathbf{q}}(\omega)\tilde{\Pi}^{R/A}_{\lambda\mathbf{q}}(\omega)\mathcal{B}^{R/A}_{\lambda\mathbf{q}}(\omega). \tag{18}$$

At this point it is important to note that, although the Dyson equation with a first-order self-energy [as in Eq. (14)] can give in principle an accurate description of the QP properties such as QP energy and lifetime, it does not correctly reproduce the position of the satellites. Indeed, several calculations of the one-particle G demonstrated that satellites associated to one-plasmon [52–58] or one-phonon [25,26] scattering processes are better described through a second-order expansion in terms of the particle-boson coupling in which the starting Green's function already contains QP effects rather than a full iterative scheme starting from noninteracting Green's function such as in Eq. (14). In the following, in order to provide an adequate treatment of both QP and one-phonon satellites, we extend the approach developed by Bechstedt *et al.* [58] for the description of plasmonic satellites in the context of one-particle excitations to the case of the exciton propagator. First of all, we cut the exciton self-energy in two parts: a QP contribution $\tilde{\Pi}^{R/A}_{\lambda\mathbf{q}}(E^{QP}_{\lambda\mathbf{q}})$ evaluated at the exciton QP energy $(E^{QP}_{\lambda\mathbf{q}})$, and a dynamical contribution $\Delta\tilde{\Pi}_{\lambda\mathbf{q}}(\omega) = \tilde{\Pi}_{\lambda\mathbf{q}}(\omega) - \tilde{\Pi}^{R/A}_{\lambda\mathbf{q}}(E^{QP}_{\lambda\mathbf{q}})$. Thus by definition $\Delta\tilde{\Pi}^{\lessgtr}_{\lambda\mathbf{q}}(\omega) \approx \tilde{\Pi}^{\lessgtr}_{\lambda\mathbf{q}}(\omega)$. Then we expand $\mathcal{B}$ at the first order in $\Delta\tilde{\Pi}$,

$$\begin{aligned}\mathcal{B}^{\lessgtr}_{\lambda\mathbf{q}}(\omega) = {}& \mathcal{B}^{QP\lessgtr}_{\lambda\mathbf{q}}(\omega) + \mathcal{B}^{QP\lessgtr}_{\lambda\mathbf{q}}(\omega)\Delta\tilde{\Pi}^{A}_{\lambda\mathbf{q}}(\omega)\mathcal{B}^{QPA}_{\lambda\mathbf{q}}(\omega) \\ & + \mathcal{B}^{QPR}_{\lambda\mathbf{q}}(\omega)\tilde{\Pi}^{\lessgtr}_{\lambda\mathbf{q}}(\omega)\mathcal{B}^{QPA}_{\lambda\mathbf{q}}(\omega) \\ & + \mathcal{B}^{QPR}_{\lambda\mathbf{q}}(\omega)\Delta\tilde{\Pi}^{R}_{\lambda\mathbf{q}}(\omega)\mathcal{B}^{QP\lessgtr}_{\lambda\mathbf{q}}(\omega),\end{aligned} \tag{19}$$

$\mathcal{B}^{QP}$ being the QP exciton propagator defined by the following equation:

$$\mathcal{B}^{QPR/A}_{\lambda\mathbf{q}}(\omega) = \bar{\mathcal{B}}^{R/A}_{\lambda\mathbf{q}}(\omega) + \bar{\mathcal{B}}^{R/A}_{\lambda\mathbf{q}}(\omega)\tilde{\Pi}^{R/A}_{\lambda\mathbf{q}}\left(E^{QP}_{\lambda\mathbf{q}}\right)\mathcal{B}^{QPR/A}_{\lambda\mathbf{q}}(\omega). \tag{20}$$

In practice, $\mathcal{B}^{QP}$ is obtained replacing $E_{\lambda\mathbf{q}}$ with $E^{QP}_{\lambda\mathbf{q}}$ in the expression of $\bar{\mathcal{B}}$. The QP energy, according to Eq. (20), is obtained through the self-consistent relation $E^{QP}_{\lambda\mathbf{q}} = E_{\lambda\mathbf{q}} + \mathrm{Re}\tilde{\Pi}^{R/A}_{\lambda\mathbf{q}}(E^{QP}_{\lambda\mathbf{q}})$. Finally inserting the explicit expression of the exciton and phonon Green's functions in Eq. (19), the lesser part of $\mathcal{B}$ that gives direct access to the photoluminescence spectra can be written as

$$\begin{aligned}\mathcal{B}^{<}_{\lambda\mathbf{q}=0}(\omega) = -2i\pi\Bigg[& f_{\lambda\mathbf{q}=0}(1-R_{\lambda\mathbf{q}=0})\delta\left(\omega - E^{QP}_{\lambda\mathbf{q}=0}\right) \\ & + \frac{1}{N}\sum_{\alpha\mu\bar{\mathbf{q}}}\frac{f_{\alpha\bar{\mathbf{q}}}(N_{\mu\bar{\mathbf{q}}}+1)\left|g^{\mathrm{exc}}_{\alpha\lambda;\mu}(0\bar{\mathbf{q}})\right|^2}{\left[E^{QP}_{\lambda\mathbf{q}=0} - \Omega^{-}_{\alpha\mu}(\bar{\mathbf{q}})\right]^2}\delta(\omega - \Omega^{-}_{\alpha\mu}(\bar{\mathbf{q}})) \\ & + \frac{1}{N}\sum_{\alpha\mu\bar{\mathbf{q}}}\frac{f_{\alpha\bar{\mathbf{q}}}N_{\mu\bar{\mathbf{q}}}\left|g^{\mathrm{exc}}_{\alpha\lambda;\mu}(0\bar{\mathbf{q}})\right|^2}{\left[E^{QP}_{\lambda\mathbf{q}=0} - \Omega^{+}_{\alpha\mu}(\bar{\mathbf{q}})\right]^2}\delta(\omega - \Omega^{+}_{\alpha\mu}(\bar{\mathbf{q}}))\Bigg],\end{aligned} \tag{21}$$

where we introduced the quantity $\Omega^{\pm}_{\alpha\mu}(\bar{\mathbf{q}}) = E_{\alpha\bar{\mathbf{q}}} \pm \Omega_{\mu\bar{\mathbf{q}}}$ with $\Omega_{\mu\mathbf{q}}$ denoting the phonon frequencies, $N_{\mu\mathbf{q}}$ the phonon occupation numbers and $f_{\lambda\mathbf{q}}$ the exciton occupation numbers defined in Appendix B. The quantity $R_{\lambda\mathbf{q}}$ indicates the renormalization factor

$$R_{\lambda\mathbf{q}} = -\frac{\partial}{\partial\omega}\mathrm{Re}\tilde{\Pi}^{R/A}_{\lambda\mathbf{q}}(\omega)|_{\omega=E^{QP}_{\lambda\mathbf{q}}} \tag{22}$$

and allows to quantify the amount of spectral weight transferred from the QP peak [first term in Eq. (21)] to the satellites. The latter are associated to optical transitions accompanied by the emission or absorption of a phonon and are described by the second and third term of Eq. (21), respectively. For simplicity, in Eq. (21) we neglect the finite linewidth (or exciton lifetime) induced by the exciton-phonon coupling. Nevertheless, this quantity can be directly obtained from the exciton self-energy through the relation $\Gamma_{\lambda\mathbf{q}} = \mp\mathrm{Im}\tilde{\Pi}^{R/A}_{\lambda\mathbf{q}}(\omega)|_{\omega=E^{QP}_{\lambda\mathbf{q}}}$.

The expression of the satellite structures in Eq. (21) is similar to that obtained with a phenomenological approach in previous papers [16,17]. The basic difference is that here we take into account QP energy corrections and the renormalization factor that are missing in previous approaches. In this way we treat QP excitations and satellites on the same footing. In addition, the present approach can be applied for arbitrary nonthermal distribution involving also high density of photo-excited carriers characterized by inversion of population. However, in this case one should consider the full expression of the exciton self-energy as detailed in Appendix A.

B. Multiphonon processes from a Cumulant expansion

The analysis done so far has shown how dynamical effects on the spectra of neutral excitations can be included solving an approximate one-particle Dyson equation for the exciton propagator where dynamical effects beyond the SBSE are taken into account through an effective exciton self-energy. The latter is evaluated at the first order in the dynamical exciton-exciton interaction ($\mathcal{W}$) and reflects a picture of an effective particle (the exciton) coupled with an effective bosonic field in analogy with the GW (or GW$^{\mathrm{ph}}$) self-energy in the case of one-electron Green's function. As a matter of fact the GW approximation for the one-electron Green's function represents the leading-order solution of a particle-boson Hamiltonian. In the present case the particle is represented by the exciton instead of the electron. In the case of one-electron Green's function, a well-established scheme to deal with this problem beyond the GW approximation is the linked-cluster (or cumulant) expansion of G [59]. Here we assume that the standard series expansion of G in terms of W obtained from the Feynman diagrams can be regrouped as an exponential power series in W, $G = G_0 e^C$ with $C = \sum_i C_i$. C_i being the cumulant coefficients evaluated at the ith order in W and G_0 the noninteracting one-electron Green's function. The coefficients C_i are found by equating terms with like powers of W in the standard series expansions of G. Although, in principle, they can be evaluated at any order, in practice we truncate C at the first order in W (i.e., we take $C = C_1$). This approximation gives an accurate description of both plasmon and phonon satellites in the photoemission spectra. Originally formulated for the time-ordered G [60–62], the cumulant approach has been extended to other correlation functions involving the retarded G [63,64] as well as the nonequilibrium Green's functions on the Keldysh contour [65].

Thus, following the analogy with the one-electron Green's function, a natural way to treat dynamical effects beyond the first-order $\mathcal{W}$ in the spectra of neutral excitations, is to perform a cumulant expansion for the exciton propagator. To this end, we take the assumption that $\tilde{\Pi}$ is diagonal in the basis of the excitonic states and we consider the following ansatz for the symmetrized exciton propagator:

$$\mathcal{B}^{\lessgtr}_{\lambda\mathbf{q}}(t) = \mathcal{B}^{QP\lessgtr}_{\lambda\mathbf{q}}(t)e^{C^{\lessgtr}_{\lambda\mathbf{q}}(t)} \tag{23}$$

where $C^{\lessgtr}_{\lambda\mathbf{q}}(t)$ is evaluated at the first order in $\mathcal{W}$. Finally, comparison of the first-order C expansion of Eq. (23) with Eq. (19) leads an explicit expression of the cumulant coefficient in terms of the exciton self-energy,

$$C^{\lessgtr}_{\lambda\mathbf{q}}(t) = R_{\lambda\mathbf{q}} + \tilde{C}^{\lessgtr}_{\lambda\mathbf{q}}(t), \tag{24}$$

where $R_{\lambda\mathbf{q}}$ is the renormalization factor given by Eq. (22) and $\tilde{C}^{\lessgtr}_{\lambda\mathbf{q}}(t)$ describes the satellite structures as

$$\tilde{C}^{\lessgtr}_{\lambda\mathbf{q}}(t) = \frac{i}{f^{\lessgtr}_{\lambda\mathbf{q}}}\int_{-\infty}^{\infty}\frac{d\omega}{2\pi}\frac{\tilde{\Pi}^{\lessgtr}_{\lambda\mathbf{q}}\left(\omega + E^{QP}_{\lambda\mathbf{q}}\right)}{\omega^2+\eta^2}e^{i\omega t}, \tag{25}$$

with $f^{<}_{\lambda\mathbf{q}} = f_{\lambda\mathbf{q}}$ and $f^{>}_{\lambda\mathbf{q}} = 1 + f_{\lambda\mathbf{q}}$. Equation (23) together with Eqs. (24) and (25) is formally exact in the limiting case of a single exciton with infinite mass coupled with a nondispersive boson and represents the generalization to the

out-of-equilibrium conditions of the standard cumulant for the time-ordered exciton propagator [20,21].

V. APPLICATION TO A SIMPLE MODEL SYSTEM

Below, as an illustrative example, we consider a simple model system consisting of a single Wannier exciton coupled with an Einstein-like longitudinal optical (LO) phonon of frequency Ω_0 and a longitudinal acoustic (LA) phonon with linear dispersion. Moreover, we model the coupling with the LO phonon through a long-range Fröhlich-like electron-phonon interaction [66] while for the LA phonon we use a short-range coupling linear in the phonon wave vector q [67]. Under these conditions the exciton-phonon matrix elements in Eq. (16) have a simple analytical expression in terms of the exciton Bohr radius (a) and the electron and hole masses (see Appendix C),

$$\left|g^{\rm exc}_{LO}(\mathbf{q}=0,\bar{\mathbf{q}})\right|^2 = \alpha_{LO}\Omega_0^2\frac{[I_c(|\bar{\mathbf{q}}|)-I_v(|\bar{\mathbf{q}}|)]^2}{|\mathbf{q}|^2}, \quad (26)$$

$$\left|g^{\rm exc}_{LA}(\mathbf{q}=0,\bar{\mathbf{q}})\right|^2 = \alpha_{LA}\Omega_D^2|\bar{\mathbf{q}}|[I_c(|\bar{\mathbf{q}}|)-I_v(|\bar{\mathbf{q}}|)]^2, \quad (27)$$

with

$$I_{c(v)}(q) = \frac{1}{\left[1+\left(\frac{m_{c(v)}}{M}\frac{|\bar{\mathbf{q}}|a}{2}\right)^2\right]^2}. \quad (28)$$

Here α_{LO} and α_{LA} are dimensionless constants, $|\bar{\mathbf{q}}|$ is expressed in unit of the Debye wave vector q_D, Ω_D is the Debye frequency, $m_{c(v)}$ are the effective mass of the conduction and valence band, respectively, and $M = m_c + m_v$ the exciton mass. In addition we take the assumption that the system is in a quasi-equilibrium configuration so that the exciton occupation numbers are Bose-Einstein distributions with chemical potential $\mu_{\rm exc} = \mu_c - \mu_v$. The quantities μ_c and μ_v are the chemical potentials for electrons and holes in the conduction and valence band, respectively and for a given temperature (T) they are set by the density of photo excited carriers.

The resulting exciton self-energy has the following expression:

$$\tilde{\Pi}^<_{\mathbf{q}=0}(\omega) = -6\pi i\sum_\mu\int_0^1 d\bar{q}\bar{q}^2\left|g^{\rm exc}_\mu(\mathbf{q}=0,\bar{q})\right|^2 f_{\bar{q}} \times[(N_{\mu\bar{q}}+1)\delta(\omega-E_{\bar{q}}+\Omega_{\mu\bar{q}}) + N_{\mu\bar{q}}\delta(\omega-E_{\bar{q}}-\Omega_{\mu\bar{q}})], \quad (29)$$

where μ runs over the LA and LO branches, $\Omega_{LO\bar{q}} = \Omega_0$, and $\Omega_{LA\bar{q}} = \Omega_D\bar{q}$. Finally under the assumption that the density of photo-excited carriers is small enough, we can neglect the effect of the Pauli blocking factor ($R_{\rm cv} \approx 1$) and safely take $\mathcal{P}^<_{\lambda\lambda'} = \mathcal{B}^<_\lambda\delta_{\lambda\lambda'}$.

In Fig. 3 we show the exciton self-energy as a function of the frequency with the origin set to the value of the direct exciton energy ($E_{\bar{q}=0}$). The coupling with the nondispersive LO phonon gives rise to two well-defined peaks located at $\omega = \pm\Omega_0$ that dominate the behavior of the exciton self-energy due to the long-range nature of $g^{\rm exc}_{LO}$. On the other hand, the coupling with the LA phonon is in general weaker due to the excitonic effect that, through the factor $I_{c(v)}$, kills the exciton-phonon coupling at $q \gg \frac{2\pi}{a}$.

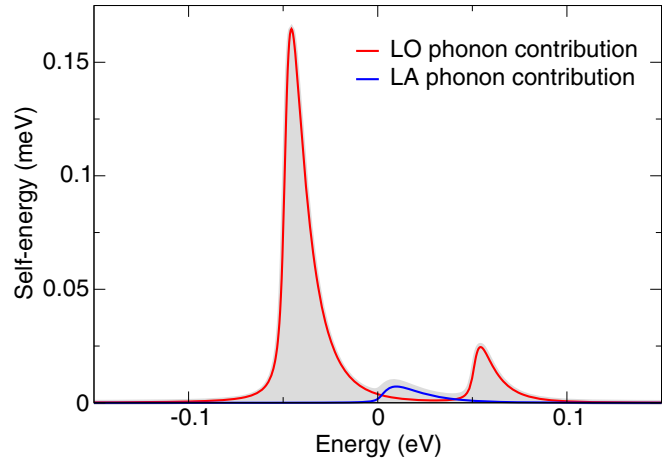

FIG. 3. Lesser component of the exciton self-energy evaluated a $T = 300$ K. The gray region defines the full spectrum while the red and blue lines the contributions of the LO and LA phonons, respectively.

In this way only the small long-range part of the electron-phonon interaction contribute to build $g^{\rm exc}_{LA}$. The dominant contribution of the long-range part of the exciton-phonon coupling also justifies the use of the Einstein and Debye models for the LO and LA phonons, respectively, making this simple model a reliable picture of the basic phenomenology of polar crystals. Moreover, at variance with the LO phonon, the coupling with the LA phonon does not lead to well-defined peaks in the spectrum of $\Pi^<(\omega)$ but it only induces a small shoulder close to the exciton energy. This is strictly related to the linear dispersion of the acoustic phonon. From this analysis of the exciton self-energy we can conclude that in this model system only the coupling with LO phonon can induce satellites in the PL spectra. On the other hand, since the contributions of the LO and the LA phonons to the exciton self-energy remain finite at the exciton energy, both phonon branches contribute to the exciton linewidth.

Insertion of Eq. (29) into Eq. (25) allows to evaluate the cumulant coefficient and through the Fourier transform of Eq. (23), the PL spectra. Our results are summarized in Fig. 4 where we show the PL spectra (blue line) for different temperatures. The coupling with the LO phonon gives rise to two main effects: the appearance of a series of satellites at energies $E^{QP} \pm n\Omega_0$ with integer n, and a weight transfer from the QP peak to the satellites that is quantified by the renormalization factor appearing in the definition of the cumulant coefficient. The structure of the satellite features can be qualitatively understood in the limiting case of an exciton with infinite mass coupled through a q-independent exciton-phonon coupling constant g. In this case the integral in Eq. (25) can be performed analytically leading to the following expression for $\mathcal{B}^<(\omega)$:

$$\mathcal{B}^<(\omega) = -2\pi i e^{-R}\sum_{n,m=0}^{\infty}\beta_{mn}\delta(\omega-E_m+n\Omega_0), \quad (30)$$

where $R = (\frac{g}{\Omega_0})^2(2N+1)$ is the renormalization factor, $E_m = E_0 + m\Omega_0$ (E_0 being the exciton energy), and the coefficient

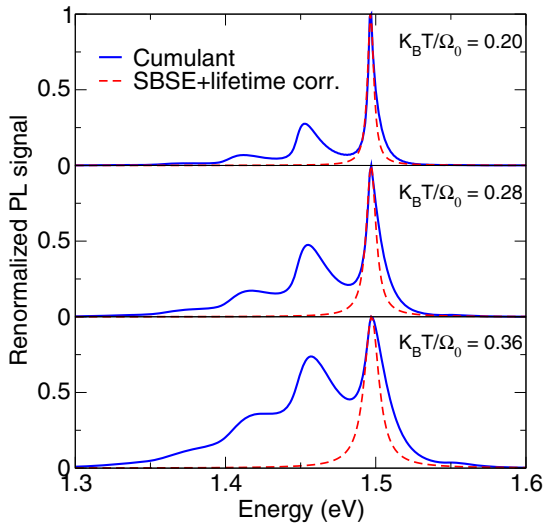

FIG. 4. Model PL spectra renormalized to the strength of the QP peaks evaluated in different approximations.

β_{mn} are defined as

$$\beta_{mn} = \frac{\left[\left(\frac{g}{\Omega_0}\right)^2 N\right]^m}{m!} \frac{\left[\left(\frac{g}{\Omega_0}\right)^2 (N+1)\right]^n}{n!}. \tag{31}$$

The phonon side bands with $m = 0$ define the Stokes lines (SLs) of the spectrum. Their intensity relative to the zero phonon line at E_0 follows a Poisson distribution as predicted by the Huang-Rhys theory [68,69]. Indeed, the quantity in Eq. (31) taken at $m = 0$ is just the Huang-Rhys factor that in state-of-the-art *ab initio* calculations can be also evaluated combining configuration coordinate models and DFT [70]. In a polaronic picture, where E_m have the physical meaning of exciton-polaron energy levels, the SLs correspond to the components with n LO phonons of the ground-state exciton-polaron ($m = 0$). Furthermore, the excited exciton-polaron states (configurations with $m > 0$), which are not handled in the Huang-Rhys theory, can produce anti-Stokes lines (ASLs) by their components with phonon number $n < m$. Other components with $n \geqslant m$ will intensify the zero phonon line and corresponding SLs. All these effects are correctly described by the cumulant according with the polaronic model that in this limit is formally exact and is often used to describe phonon assisted PL spectra arising from excitons bound to impurities [71–73]. The effect of exciton dispersion, as can be inferred from Fig. 4, is to change the shape of the phonon side bands inducing a broadening of the corresponding peak, which depends from the details of the exciton and phonon band structure as well as the behavior of the exciton-phonon matrix elements.

It is important to note that beside satellites, the cumulant expansion takes into account the finite exciton lifetime as well, as can be inferred from Fig. 4, where the QP peak progressively broadens as T increases. This can be directly understood from the definition of the cumulant coefficient. Indeed taking the QP approximation in Eq. (25), i.e., keeping $\Pi^<$ at the corresponding value of the exciton QP energy over all the integration region, we obtain $\tilde{C}_{\lambda\mathbf{q}}(t) = -\frac{i\Pi^<_{\lambda\mathbf{q}}(E^{QP}_{\lambda\mathbf{q}})}{2f_{\lambda\mathbf{q}}}|t|$. From the definition of $\Pi^<_{\lambda\mathbf{q}}(\omega)$ we can verify that in the limit of small density of photo-excited carriers $\frac{i\Pi^<_{\lambda\mathbf{q}}(E^{QP}_{\lambda\mathbf{q}})}{2f_{\lambda\mathbf{q}}} \approx \Gamma_{\lambda\mathbf{q}}$ ($\Gamma_{\lambda\mathbf{q}}$ being the exciton linewidth defined in the previous section).

Finally, in Fig. 4 we make a comparison with the PL spectra evaluated in the QP approximation (dashed red line). They are obtained from the SBSE spectra corrected with exciton linewidth, i.e., taking for $\mathcal{B}^<_{\lambda\mathbf{q}}(\omega)$ the following expression:

$$\mathcal{B}^<_{\lambda\mathbf{q}}(\omega) = -\frac{2i\Gamma_{\lambda\mathbf{q}}}{(\omega - E_{\lambda\mathbf{q}})^2 + \Gamma^2_{\lambda\mathbf{q}}}. \tag{32}$$

Interestingly, as T increases, the QP peak obtained in the cumulant approximation progressively depart from the Lorentzian shape of Eq. (32) displaying a transfer of spectral weight towards the right side of the QP energy. This behavior is tightly linked to the presence of a low-energy shoulder in spectrum of the exciton self-energy (see blue-line in Fig. 3) induced by the coupling with the LA phonon. As T increases, this feature becomes more pronounced due to the higher phonon population and the asymmetry of the QP peak is enhanced. We emphasize that this effect becomes more evident as the shoulder moves away from the QP energy. This could happen in multivalley semiconductors, where higher energy acoustic phonons can mediate intervalley exciton scattering, as recently observed in the PL spectra of monolayer transition metal dichalcogenides [74,75].

VI. CONCLUSIONS

In conclusion, starting from basic equations of MBPT, we have generalized the cumulant formulation for neutral excitation spectra to the calculation of the out-of-equilibrium polarizability that gives direct access to the PL spectra. The cumulant approach allows us to include dynamical effects arising from the electronic correlation and electron-phonon coupling in a simple and intuitive way. It can be implemented as a postprocessing of a standard out-of-equilibrium BSE calculation of excitonic states and real-time relaxation of photo-excited carriers.

ACKNOWLEDGMENT

This research was supported by the Fonds National de Recherche (FNR), Luxembourg, via Project No. INTER/19/ANR/13376969/ACCEPT.

APPENDIX A: EXCITON SELF-ENERGY IN THE BASIS OF BLOCH STATES

Here, skipping the intermediate steps of elementary algebra, we report the explicit expression of the exciton self-energy in the basis of Bloch states that can be directly read from the right side of Fig. 2. It is the sum of a static (${}^s\Pi$)

and a full dynamical ($^d\Pi$) contribution as detailed below:

$$
\begin{aligned}
{}^s\Pi^{\mathbf{cv}}_{\mathbf{c'v'}}(z_{13}) = -\frac{1}{R_{\mathbf{cv}}}\Big\{ & \frac{1}{2}\delta_{\mathbf{vv'}}\delta(z_{13})\big[W^{\mathbf{cc'}}_{\mathbf{ii}}\cdot i\mathcal{P}^{\mathbf{ci}}_0\big](z_{31}) + \frac{1}{2}\delta_{\mathbf{vv'}}\delta(z_{13})\big[i\mathcal{P}^{\mathbf{c'i}}_0\cdot W^{\mathbf{cc'}}_{\mathbf{ii}}\big](z_{31}) \\
& + \frac{1}{2}\delta_{\mathbf{cc'}}\delta(z_{13})\big[W^{\mathbf{jj}}_{\mathbf{v'v}}\cdot i\mathcal{P}^{\mathbf{jv}}_0\big](z_{31}) + \frac{1}{2}\delta_{\mathbf{cc'}}\delta(z_{13})\big[i\mathcal{P}^{\mathbf{jv'}}_0\cdot W^{\mathbf{jj}}_{\mathbf{v'v}}\big](z_{31})\Big\}\frac{1}{R_{\mathbf{c'v'}}}, \qquad \text{(A1)}
\end{aligned}
$$

$$
\begin{aligned}
{}^d\Pi^{\mathbf{cv}}_{\mathbf{c'v'}}(z_{13}) = \frac{1}{R_{\mathbf{cv}}}\Big\{ & i\bar{\mathcal{P}}^{\mathbf{iv}}_{\mathbf{jv'}}(z_{13})W^{\mathbf{cc'}}_{\mathbf{ji}}(z_{31}) + i\bar{\mathcal{P}}^{\mathbf{lv}_1}_{\mathbf{mv}_2}(z_{13})\Xi^{\mathbf{iv}}_{s\mathbf{lv}_1}\big[i\mathcal{P}^{\mathbf{c'j}}_0\cdot W^{\mathbf{cc'}}_{\mathbf{ji}}\cdot i\mathcal{P}^{\mathbf{ci}}_0\big](z_{31})\Xi^{\mathbf{mv}_2}_{s\mathbf{jv'}} \\
& - i\bar{\mathcal{P}}^{\mathbf{l\bar{v}}}_{\mathbf{jv'}}(z_{13})\Xi^{\mathbf{iv}}_{s\mathbf{l\bar{v}}}\big[W^{\mathbf{cc'}}_{\mathbf{ji}}\cdot i\mathcal{P}^{\mathbf{ci}}_0\big](z_{31}) - i\bar{\mathcal{P}}^{\mathbf{iv}}_{\mathbf{l\bar{v}}}(z_{13})\big[i\mathcal{P}^{\mathbf{c'j}}_0\cdot W^{\mathbf{cc'}}_{\mathbf{ji}}\big](z_{31})\Xi^{\mathbf{l\bar{v}}}_{s\mathbf{jv'}} \\
& - i\bar{\mathcal{P}}^{\mathbf{\bar{c}v}}_{\mathbf{c'\bar{v}}}(z_{13})W^{\mathbf{c\bar{v}}}_{\mathbf{v'\bar{c}}}(z_{31}) - i\bar{\mathcal{P}}^{\mathbf{c}_1\mathbf{v}_1}_{\mathbf{c}_2\mathbf{v}_2}(z_{13})\Xi^{\mathbf{\bar{c}v}}_{s\mathbf{c}_1\mathbf{v}_1}\big[i\mathcal{P}^{\mathbf{\bar{v}v'}}_0\cdot W^{\mathbf{c\bar{v}}}_{\mathbf{v'\bar{c}}}\cdot i\mathcal{P}^{\mathbf{c\bar{c}}}_0\big](z_{31})\Xi^{\mathbf{c}_2\mathbf{v}_2}_{s\mathbf{c'\bar{v}}} \\
& + i\bar{\mathcal{P}}^{\mathbf{c}_1\mathbf{v}_1}_{\mathbf{c'\bar{v}}}(z_{13})\Xi^{\mathbf{\bar{c}v}}_{s\mathbf{c}_1\mathbf{v}_1}\big[W^{\mathbf{c\bar{v}}}_{\mathbf{v'\bar{c}}}\cdot i\mathcal{P}^{\mathbf{c\bar{c}}}_0\big](z_{31}) + i\bar{\mathcal{P}}^{\mathbf{\bar{c}v}}_{\mathbf{c}_1\mathbf{v}_1}(z_{13})\big[i\mathcal{P}^{\mathbf{\bar{v}v'}}_0\cdot W^{\mathbf{c\bar{v}}}_{\mathbf{v'\bar{c}}}\big](z_{31})\Xi^{\mathbf{c}_1\mathbf{v}_1}_{s\mathbf{c'\bar{v}}} \\
& + i\bar{\mathcal{P}}^{\mathbf{ci}}_{\mathbf{c'j}}(z_{13})W^{\mathbf{ij}}_{\mathbf{v'v}}(z_{31}) + i\bar{\mathcal{P}}^{\mathbf{c}_1\mathbf{l}}_{\mathbf{c}_2\mathbf{m}}(z_{13})\Xi^{\mathbf{ci}}_{s\mathbf{c}_1\mathbf{l}}\big[i\mathcal{P}^{\mathbf{jv'}}_0\cdot W^{\mathbf{ij}}_{\mathbf{v'v}}\cdot i\mathcal{P}^{\mathbf{iv}}_0\big](z_{31})\Xi^{\mathbf{c}_2\mathbf{m}}_{s\mathbf{c'j}} \\
& - i\bar{\mathcal{P}}^{\mathbf{\bar{c}l}}_{\mathbf{c'j}}(z_{13})\Xi^{\mathbf{ci}}_{s\mathbf{\bar{c}l}}\big[W^{\mathbf{ij}}_{\mathbf{v'v}}\cdot i\mathcal{P}^{\mathbf{iv}}_0\big](z_{31}) - i\bar{\mathcal{P}}^{\mathbf{ci}}_{\mathbf{\bar{c}l}}(z_{13})\big[i\mathcal{P}^{\mathbf{jv'}}_0\cdot W^{\mathbf{ij}}_{\mathbf{v'v}}\big](z_{31})\Xi^{\mathbf{\bar{c}l}}_{s\mathbf{c'j}} \\
& - i\bar{\mathcal{P}}^{\mathbf{c\bar{v}}}_{\mathbf{\bar{c}v'}}(z_{13})W^{\mathbf{\bar{v}c'}}_{\mathbf{\bar{c}v}}(z_{31}) - i\bar{\mathcal{P}}^{\mathbf{c}_1\mathbf{v}_1}_{\mathbf{c}_2\mathbf{v}_2}(z_{13})\Xi^{\mathbf{c\bar{v}}}_{s\mathbf{c}_1\mathbf{v}_1}\big[i\mathcal{P}^{\mathbf{c'\bar{c}}}_0\cdot W^{\mathbf{\bar{v}c'}}_{\mathbf{\bar{c}v}}\cdot i\mathcal{P}^{\mathbf{\bar{v}v}}_0\big](z_{31})\Xi^{\mathbf{c}_2\mathbf{v}_2}_{s\mathbf{\bar{c}v'}} \\
& + i\bar{\mathcal{P}}^{\mathbf{c}_1\mathbf{v}_1}_{\mathbf{\bar{c}v'}}(z_{13})\Xi^{\mathbf{c\bar{v}}}_{s\mathbf{c}_1\mathbf{v}_1}\big[W^{\mathbf{\bar{v}c'}}_{\mathbf{\bar{c}v}}\cdot i\mathcal{P}^{\mathbf{\bar{v}v}}_0\big](z_{31}) + i\bar{\mathcal{P}}^{\mathbf{c\bar{v}}}_{\mathbf{c}_1\mathbf{v}_1}(z_{13})\big[i\mathcal{P}^{\mathbf{c'\bar{c}}}_0\cdot W^{\mathbf{\bar{v}c'}}_{\mathbf{\bar{c}v}}\big](z_{31})\Xi^{\mathbf{c}_1\mathbf{v}_1}_{s\mathbf{\bar{c}v'}}\Big\}\frac{1}{R_{\mathbf{c'v'}}}, \qquad \text{(A2)}
\end{aligned}
$$

with the following definition of the matrix elements between Bloch states of the correlation functions and effective interactions:

$$
\mathcal{P}^{\mathbf{ij}}_{\mathbf{lm}}(z_{13}) = \int d\mathbf{r}_{1423}\phi^*_{\mathbf{i}}(\mathbf{r}_1)\phi^*_{\mathbf{m}}(\mathbf{r}_4)\mathcal{P}(\mathbf{r}_1z_1,\mathbf{r}_4z_3,\mathbf{r}_2z_1,\mathbf{r}_3z_3)\phi_{\mathbf{l}}(\mathbf{r}_3)\phi_{\mathbf{j}}(\mathbf{r}_2), \qquad \text{(A3)}
$$

$$
W^{\mathbf{ij}}_{\mathbf{lm}}(z_{31}) = \int d\mathbf{r}_{13}\phi^*_{\mathbf{i}}(\mathbf{r}_1)\phi^*_{\mathbf{l}}(\mathbf{r}_3)W(\mathbf{r}_3z_3,\mathbf{r}_1z_1)\phi_{\mathbf{j}}(\mathbf{r}_3)\phi_{\mathbf{m}}(\mathbf{r}_1), \qquad \text{(A4)}
$$

$$
\Xi^{\mathbf{ij}}_{s\mathbf{lm}} = \int d\mathbf{r}_{1423}\phi^*_{\mathbf{i}}(\mathbf{r}_1)\phi^*_{\mathbf{m}}(\mathbf{r}_4)\Xi_s(\mathbf{r}_1,\mathbf{r}_4,\mathbf{r}_2,\mathbf{r}_3)\phi_{\mathbf{l}}(\mathbf{r}_3)\phi_{\mathbf{j}}(\mathbf{r}_2), \qquad \text{(A5)}
$$

and similarly for $\mathcal{P}^{\mathbf{ij}}_0(z_{13}) = \mathcal{P}^{\mathbf{ij}}_{0\mathbf{lm}}(z_{13})\delta_{\mathbf{il}}\delta_{\mathbf{jm}}$.

Here we use the compact notation $\mathbf{i} = (i, \mathbf{k}_i)$ to indicate, for a given Bloch state, the band index i and the corresponding wave vector $\mathbf{k}_i$ and the usual convention that repeated indexes are summed up. Moreover the indexes $\mathbf{i}$, $\mathbf{j}$, $\mathbf{l}$, and $\mathbf{m}$ in Eq. (A2) run over conduction and valence states with the constrain that they always belong to the same subset of states. This is a consequence of the TDA used for the solution of the SBSE. In particular, the first two lines of Eq. (A2), where W enters as a hole-hole interaction, correspond to the diagrams on the right side of Fig. 2(a) while line three and four correspond to the right side of Fig. 2(b) where W enters as an electron-hole interaction. The remaining terms are associated to complementary diagrams (not shown) involving electron-electron and hole-electron interaction, respectively. The static part of the self-energy, on the other hand, is related to the diagrams on right side of Fig. 2(a) and their counterpart involving electron-electron scattering processes evaluated at the zero order in the static interaction Ξ_s.

A first look to Eqs. (A1) and (A2) reveals how the different contributions to the exciton self-energy can be grouped in two classes: (i) excitonic contributions, which can be expressed solely in terms of exciton propagators as $\bar{\mathcal{P}}W$-like products; (ii) nonexcitonic contributions that cannot be expressed in terms of excitonic propagators. Indeed, while in the excitonic contributions the interaction is set by W, in the nonexcitonic contributions it is related to convolutions involving W and $\mathcal{P}_0$ (i.e., the independent particle two-time polarizability). We emphasize that the presence of nonexcitonic terms arises from the definition of the kernel $\mathcal{K}$ in Eq. (8) where W enters as test-particle-test-particle interaction. As a matter of fact the inclusion of vertex corrections (treated at the SBSE level) would lead to an expression of the exciton self-energy formally equivalent to Eqs. (A1) and (A2) but with $\mathcal{P}_0$ replaced by $\bar{\mathcal{P}}$. However, this goes beyond the aim of the present paper.

It is important to note that both quantities $\bar{\mathcal{P}}$ and $\mathcal{P}_0$ in Eqs. (A1) and (A2) involve pairs of electrons and holes belonging to the conduction and valence bands, respectively as well as electron-hole pairs belonging to the conduction or valence sub-bands. The latter are absent under equilibrium conditions and in general give a minor contribution as long as the density of photo-excited carriers is small enough. In the following we take the assumption that this

is the case and we neglect contributions arising from subband electron-hole pairs. Under these conditions Eq. (A2) simplifies and reduces to the sum of excitonic contributions only,

$$ {}^{d}\Pi^{\mathbf{cv}}_{\mathbf{c'v'}}(z_{13}) = \frac{1}{R_{\mathbf{cv}}}\left\{ i\bar{\mathcal{P}}^{\mathbf{c_1v}}_{\mathbf{c_2v'}}(z_{13})W^{\mathbf{cc'}}_{\mathbf{c_2c_1}}(z_{31}) + i\bar{\mathcal{P}}^{\mathbf{cv_1}}_{\mathbf{c'v_2}}(z_{13})W^{\mathbf{v_1v_2}}_{\mathbf{v'v}}(z_{31}) - i\bar{\mathcal{P}}^{\mathbf{c\bar{v}}}_{\mathbf{c'\bar{v}}}(z_{13})W^{\mathbf{c\bar{v}}}_{\mathbf{v'\bar{c}}}(z_{31}) - i\bar{\mathcal{P}}^{\mathbf{c\bar{v}}}_{\mathbf{\bar{c}v'}}(z_{13})W^{\mathbf{\bar{v}c'}}_{\mathbf{\bar{c}v}}(z_{31})\right\}\frac{1}{R_{\mathbf{c'v'}}}. \quad \text{(A6)} $$

Nonexcitonic terms appear only in ${}^{s}\Pi$ that in the limit of small photo excited carrier density is obtained from Eq. (A1) restricting the sum on the **i** and **j** indexes over the valence and conduction bands, respectively. In addition, since ${}^{s}\Pi$ causes only a shift of the exciton energy and does not have any effect on the exciton lifetime and satellites, we can safely take $\Pi(z_{13}) =^{d} \Pi(z_{13})$ and include ${}^{s}\Pi$ in the definition of the exciton energy.

APPENDIX B: SYMMETRIZED EXCITON PROPAGATOR AND EXCITON SELF-ENERGY

Before addressing the problem of Eq. (5), we will present a short overview of the out-of-equilibrium SBSE and its solution, which is an essential preliminary step to treat the full dynamical problem.

Since in the static limit Ξ is time independent, in analogy with the equilibrium case, Eq. (4) can be written as a Dyson like equation for the two-time polarizability $\hat{\bar{\mathcal{P}}}(z_{13}) = -i\hat{\bar{P}}(z_{1313})$ that in the following we will refer to as noninteracting exciton propagator. Thus, Eq. (4) becomes

$$ \hat{\bar{\mathcal{P}}}(z_{13}) = \hat{\mathcal{P}}_0(z_{13}) + \hat{\mathcal{P}}_0(z_{11'})i\hat{\Xi}_s\delta(z_{1'3'})\hat{\bar{\mathcal{P}}}(z_{3'3}) \quad \text{(B1)} $$

where $\hat{\mathcal{P}}_0(z_{13}) = -i\hat{P}_0(z_{1313})$ indicates the matrix associated to the uncorrelated two-time polarizability and $\hat{\Xi}_s = i\hat{W}^C_s$. Moreover under quasistationary conditions all the components of the Keldysh functions involved in Eq. (B1) depend only on the time differences. This allows solving Eq. (B1) in frequency space in analogy with what one does under equilibrium conditions [4]. In particular, Eq. (B1) can be straightforwardly treated working with a symmetrized propagator $\bar{\mathcal{B}}$ instead of $\bar{\mathcal{P}}$. In the basis of Bloch states, where $\hat{\mathcal{P}}_0$ is diagonal, it is defined in such a way that $\bar{\mathcal{P}}^{\mathbf{cv}}_{\mathbf{c'v'}}(z_{13}) = \sqrt{R_{\mathbf{cv}}}\bar{\mathcal{B}}^{\mathbf{cv}}_{\mathbf{c'v'}}(z_{13})\sqrt{R_{\mathbf{c'v'}}}$ and similarly for $\mathcal{B}_0$. Here $R_{\mathbf{cv}} = f_{\mathbf{v}} - f_{\mathbf{c}}$, $R^{<}_{\mathbf{cv}} = f_{\mathbf{c}}(1-f_{\mathbf{v}})$, and $R^{>}_{\mathbf{cv}} = (1-f_{\mathbf{c}})f_{\mathbf{v}}$ [$f_{\mathbf{c(v)}}$ being the occupation numbers for conduction (valence) states]. By definition, the propagator $\bar{\mathcal{B}}$ satisfies a SBSE equivalent to Eq. (B1) with the new symmetrized kernel $\tilde{\Xi}^{\mathbf{cv}}_{s\mathbf{c'v'}} = \sqrt{R_{\mathbf{cv}}}\Xi^{\mathbf{cv}}_{s\mathbf{c'v'}}\sqrt{R_{\mathbf{c'v'}}}$. Its solution leads to the following expression for the corresponding lesser ($<$) and greater ($>$) components [16,35]:

$$ \bar{\mathcal{B}}^{\lessgtr}_{\lambda\mathbf{q}\lambda'\mathbf{q}}(\omega) = -2i\eta\frac{1}{\omega - E_{\lambda\mathbf{q}} + i\eta}\sum_{\mathbf{cv}}A^{\mathbf{cv}}_{\lambda\mathbf{q}}\frac{R^{\lessgtr}_{\mathbf{cv}}}{R_{\mathbf{cv}}}A^{\mathbf{cv}*}_{\lambda'\mathbf{q}} \times \frac{1}{\omega - E_{\lambda'\mathbf{q}} - i\eta}, \quad \text{(B2)} $$

where $E_{\lambda\mathbf{q}}$ and $A^{\mathbf{cv}}_{\lambda\mathbf{q}}$ are the exciton energies and the corresponding eigenstates with band index λ and wave vector $\mathbf{q}$ obtained from the diagonalization of the symmetrized excitonic Hamiltonian [43]. In the TDA [39,40] it takes the following structure:

$$ \hat{H} = (\varepsilon_{\mathbf{c}} - \varepsilon_{\mathbf{v}})\delta_{\mathbf{cc'}}\delta_{\mathbf{vv'}} + i\tilde{\Xi}^{\mathbf{cv}}_{s\mathbf{c'v'}}. \quad \text{(B3)} $$

We emphasize that the Hamiltonian in Eq. (B3) is Hermitian and it is actually what is implemented in standard MBPT based codes [35]. In addition, in state-of-the-art calculations we neglect off-diagonal contributions in Eq. (B2) (i.e., we take the assumption that $\lambda = \lambda'$). Under these conditions $\bar{\mathcal{B}}$ is diagonal in the excitonic basis and the corresponding $<$ and $>$ components in real time become

$$ \bar{\mathcal{B}}^{<}_{\lambda\mathbf{q}}(t_{13}) = -if_{\lambda\mathbf{q}}e^{iE_{\lambda\mathbf{q}}(t_3-t_1)}, \quad \text{(B4)} $$

$$ \bar{\mathcal{B}}^{>}_{\lambda\mathbf{q}}(t_{13}) = -i(1+f_{\lambda\mathbf{q}})e^{iE_{\lambda\mathbf{q}}(t_3-t_1)}, \quad \text{(B5)} $$

where we have introduced the quantity $f_{\lambda\mathbf{q}} = \sum_{\mathbf{cv}}|A^{\mathbf{cv}}_{\lambda\mathbf{q}}|^2\frac{R^{\lessgtr}_{\mathbf{cv}}}{R_{\mathbf{cv}}}$ and we used the identity $R^{>}_{\mathbf{cv}} = R^{<}_{\mathbf{cv}} + R_{\mathbf{cv}}$. Now we can clearly recognize in these equations the $<$ and $>$ components of the propagator of a free boson with energy $E_{\lambda\mathbf{q}}$ and occupation number $f_{\lambda\mathbf{q}}$. Moreover through the definition of $\bar{\mathcal{B}}$ we can obtain the explicit expression of the noninteracting exciton propagator in the basis of excitonic states

$$ \bar{\mathcal{P}}_{\boldsymbol{\lambda\lambda'}}(z_{13}) = \sum_{\boldsymbol{\alpha}}F_{\boldsymbol{\lambda\alpha}}\bar{\mathcal{B}}_{\boldsymbol{\alpha}}(z_{13})F^{*}_{\boldsymbol{\lambda'\alpha}} \quad \text{(B6)} $$

with $F_{\boldsymbol{\lambda\alpha}} = \sum_{\mathbf{cv}}A^{\mathbf{cv}*}_{\boldsymbol{\lambda}}\sqrt{R_{\mathbf{cv}}}A^{\mathbf{cv}}_{\boldsymbol{\alpha}}$ and $\boldsymbol{\lambda} = (\lambda, \mathbf{q})$.

Under equilibrium conditions (i.e., in absence of population) $R_{\mathbf{cv}} = 1$ and $F_{\boldsymbol{\lambda\alpha}} = \delta_{\boldsymbol{\lambda\alpha}}$ so that the exciton behaves as an ideal boson (i.e., $\bar{\mathcal{P}}_{\boldsymbol{\lambda\lambda'}} = \bar{\mathcal{B}}_{\boldsymbol{\lambda}}\delta_{\boldsymbol{\lambda\lambda'}}$). On the other hand, out-of-equilibrium the exciton can scatter between two excitonic states even in absence of interaction. In other words it cannot be described as an ideal boson [76]. This is strictly related to the composite nature of the exciton that consists of electron-hole pairs that always follow the Pauli exclusion principle also when bound in the excitonic state. As a consequence, when an exciton propagates in presence of an exciton population it can scatter between different states through the exchange of electrons and holes with the other excitons. The amplitude of these scattering processes is set by $F_{\boldsymbol{\lambda\alpha}}$.

Finally, the full dynamical problem can be treated introducing the symmetrized full interacting exciton propagator $\mathcal{B}_{\boldsymbol{\alpha\alpha'}}$,

$$ \mathcal{P}_{\boldsymbol{\lambda\lambda'}}(z_{13}) = \sum_{\boldsymbol{\alpha\alpha'}}F_{\boldsymbol{\lambda\alpha}}\mathcal{B}_{\boldsymbol{\alpha\alpha'}}(z_{13})F^{*}_{\boldsymbol{\lambda'\alpha'}}, \quad \text{(B7)} $$

that is evaluated solving Eq. (14). From Eq. (A6) we can directly write the expression for $\tilde{\Pi}^{\mathbf{cv}}_{\mathbf{c'v'}} = \sqrt{R_{\mathbf{cv}}}\Pi^{\mathbf{cv}}_{\mathbf{c'v'}}\sqrt{R_{\mathbf{c'v'}}}$, which defines the self-energy in the Dyson equation for $\mathcal{B}$. In particular, it takes a more compact structure in the basis of the eigenstates of the symmetrized excitonic Hamiltonian,

$$ \tilde{\Pi}_{\lambda\mathbf{q}\lambda'\mathbf{q}}(z_{13}) = i\bar{\mathcal{B}}_{\alpha\mathbf{q}'}(z_{13})\mathcal{W}_{\lambda\mathbf{q}\alpha\mathbf{q}'\alpha\mathbf{q}'\lambda'\mathbf{q}}(z_{31}), \quad \text{(B8)} $$

with

$$
\begin{aligned}
&\mathcal{W}_{\lambda\mathbf{q}\alpha\mathbf{q}'\alpha\mathbf{q}'\lambda'\mathbf{q}}(z_{31}) \\
&= A^{c_1v_1\mathbf{k}_1*}_{\lambda\mathbf{q}} A^{c_2\bar{v}_2\mathbf{k}_2+\mathbf{q}-\mathbf{q}'*}_{\alpha\mathbf{q}'} \sqrt{\frac{R_{c_1\mathbf{k}_1+\mathbf{q}\bar{v}_1\mathbf{k}_1+\mathbf{q}-\mathbf{q}'}}{R_{c_1\mathbf{k}_1+\mathbf{q}v_1\mathbf{k}_1}}} W^{\bar{v}_1\mathbf{k}_1+\mathbf{q}-\mathbf{q}'\bar{v}_2\mathbf{k}_2+\mathbf{q}-\mathbf{q}'}_{v_2\mathbf{k}_2v_1\mathbf{k}_1}(z_{31}) \sqrt{\frac{R_{c_2\mathbf{k}_2+\mathbf{q}\bar{v}_2\mathbf{k}_2+\mathbf{q}-\mathbf{q}'}}{R_{c_2\mathbf{k}_2+\mathbf{q}v_2\mathbf{k}_2}}} A^{c_1\bar{v}_1\mathbf{k}_1+\mathbf{q}-\mathbf{q}'}_{\alpha\mathbf{q}'} A^{c_2v_2\mathbf{k}_2}_{\lambda'\mathbf{q}} \\
&+ A^{c_1v_1\mathbf{k}_1*}_{\lambda\mathbf{q}} A^{\bar{c}_2v_2\mathbf{k}_2*}_{\alpha\mathbf{q}'} \sqrt{\frac{R_{\bar{c}_1\mathbf{k}_1+\mathbf{q}'v_1\mathbf{k}_1}}{R_{c_1\mathbf{k}_1+\mathbf{q}v_1\mathbf{k}_1}}} W^{c_1\mathbf{k}_1+\mathbf{q}c_2\mathbf{k}_2+\mathbf{q}}_{\bar{c}_2\mathbf{k}_2+\mathbf{q}'\bar{c}_1\mathbf{k}_1+\mathbf{q}'}(z_{31}) \sqrt{\frac{R_{\bar{c}_2\mathbf{k}_2+\mathbf{q}'v_2\mathbf{k}_2}}{R_{c_2\mathbf{k}_2+\mathbf{q}v_2\mathbf{k}_2}}} A^{\bar{c}_1v_1\mathbf{k}_1}_{\alpha\mathbf{q}'} A^{c_2v_2\mathbf{k}_2}_{\lambda'\mathbf{q}} \\
&- A^{c_1v_1\mathbf{k}_1*}_{\lambda\mathbf{q}} A^{\bar{c}v_2\mathbf{k}_2*}_{\alpha\mathbf{q}'} \sqrt{\frac{R_{c_1\mathbf{k}_1+\mathbf{q}\bar{v}\mathbf{k}_1+\mathbf{q}-\mathbf{q}'}}{R_{c_1\mathbf{k}_1+\mathbf{q}v_1\mathbf{k}_1}}} W^{\bar{v}\mathbf{k}_1+\mathbf{q}-\mathbf{q}'c_2\mathbf{k}_2+\mathbf{q}}_{\bar{c}\mathbf{k}_2+\mathbf{q}'v_1\mathbf{k}_1}(z_{31}) \sqrt{\frac{R_{\bar{c}\mathbf{k}_2+\mathbf{q}'v_2\mathbf{k}_2}}{R_{c_2\mathbf{k}_2+\mathbf{q}v_2\mathbf{k}_2}}} A^{c_1\bar{v}\mathbf{k}_1+\mathbf{q}-\mathbf{q}'}_{\alpha\mathbf{q}'} A^{c_2v_2\mathbf{k}_2}_{\lambda'\mathbf{q}} \\
&- A^{c_1v_1\mathbf{k}_1*}_{\lambda\mathbf{q}} A^{c_2\bar{v}\mathbf{k}_2+\mathbf{q}-\mathbf{q}'*}_{\alpha\mathbf{q}'} \sqrt{\frac{R_{\bar{c}\mathbf{k}_1+\mathbf{q}'v_1\mathbf{k}_1}}{R_{c_1\mathbf{k}_1+\mathbf{q}v_1\mathbf{k}_1}}} W^{c_1\mathbf{k}_1+\mathbf{q}\bar{v}\mathbf{k}_2+\mathbf{q}-\mathbf{q}'}_{v_2\mathbf{k}_2\bar{c}\mathbf{k}_1+\mathbf{q}'}(z_{31}) \sqrt{\frac{R_{c_2\mathbf{k}_2+\mathbf{q}\bar{v}\mathbf{k}_2+\mathbf{q}-\mathbf{q}'}}{R_{c_2\mathbf{k}_2+\mathbf{q}v_2\mathbf{k}_2}}} A^{\bar{c}v_1\mathbf{k}_1}_{\alpha\mathbf{q}'} A^{c_2v_2\mathbf{k}_2}_{\lambda'\mathbf{q}},
\end{aligned}
\tag{B9}
$$

where we have taken into account the explicit dependence from the Bloch wave vectors.

APPENDIX C: EXCITON-PHONON MATRIX ELEMENTS

When only the electron-phonon interaction is present, $W = W^{\mathrm{ph}}$, so that, in terms of electron-phonon coupling (g) and the phonon propagator (D), Eq. (A4) becomes

$$
W^{i\mathbf{k}_i j\mathbf{k}_j}_{l\mathbf{k}_l m\mathbf{k}_m}(z_{31}) = \frac{1}{N}\sum_{\mu\mathbf{q}} g^*_{mi,\mu}(\mathbf{k}_i,\mathbf{q}) D_{\mu\mathbf{q}}(z_{31}) g_{lj,\mu}(\mathbf{k}_j,\mathbf{q}) \delta_{\mathbf{k}_m,\mathbf{k}_i+\mathbf{q}} \delta_{\mathbf{k}_l,\mathbf{k}_j+\mathbf{q}}. \tag{C1}
$$

Inserting Eqs. (C1) and (B9) into Eq. (B8) and taking the diagonal part, we obtain the expression in Eq. (16) with the following definition of the exciton-phonon matrix elements:

$$
\begin{aligned}
g^{\mathrm{exc}}_{\alpha\lambda,\mu}(\mathbf{q},\bar{\mathbf{q}}) = &\sum_{v\bar{v}c\mathbf{k}} A^{c\bar{v}\mathbf{k}-\bar{\mathbf{q}}*}_{\alpha\mathbf{q}+\bar{\mathbf{q}}} \frac{\sqrt{R_{c\mathbf{k}+\mathbf{q}\bar{v}\mathbf{k}-\bar{\mathbf{q}}}} g_{v\bar{v},\mu}(\mathbf{k}-\bar{\mathbf{q}},\bar{\mathbf{q}}) \sqrt{R_{c\mathbf{k}+\mathbf{q}v\mathbf{k}}}}{\sqrt{R_{c\mathbf{k}+\mathbf{q}v\mathbf{k}}}} A^{cv\mathbf{k}}_{\lambda\mathbf{q}} \\
&- \sum_{c\bar{c}v\mathbf{k}} A^{\bar{c}v\mathbf{k}*}_{\alpha\mathbf{q}+\bar{\mathbf{q}}} \frac{\sqrt{R_{\bar{c}\mathbf{k}+\mathbf{q}+\bar{\mathbf{q}}v\mathbf{k}}} g_{\bar{c}c,\mu}(\mathbf{k}+\mathbf{q},\bar{\mathbf{q}}) \sqrt{R_{c\mathbf{k}+\mathbf{q}v\mathbf{k}}}}{\sqrt{R_{c\mathbf{k}+\mathbf{q}v\mathbf{k}}}} A^{cv\mathbf{k}}_{\lambda\mathbf{q}}.
\end{aligned}
\tag{C2}
$$

Now we consider a simple model system consisting of a Wannier exciton coupled with an Einstein-like LO phonon of frequency $\Omega_{LO} = \Omega_0$ and LA phonon with linear dispersion $\Omega_{LA} = \varsigma|\mathbf{q}|$ with $\varsigma = \frac{\Omega_D}{q_D}$ (Ω_D and q_D being the Debye frequency and wave vector, respectively). In this case the lowest exciton energy band and the corresponding wave functions are

$$
E_{\mathbf{q}} = \Delta_{QP} - \frac{\mu}{2\epsilon^2_\infty} + \frac{q^2}{2M}, \tag{C3}
$$

$$
A^{cv\mathbf{k}}_{\mathbf{q}} = \frac{(2a)^{\frac{3}{2}}}{\pi} \frac{1}{[1+(|\mathbf{k}+\gamma\mathbf{q}|a)^2]^2}, \tag{C4}
$$

with ϵ_∞ denoting the dielectric constant of the medium, $\mu = \frac{m_c m_v}{m_c+m_v}$ the reduced mass of the electron-hole pair, $M = m_c + m_v$ the exciton mass, $a = \frac{\epsilon_\infty}{\mu}$ the exciton Bohr radius, and Δ_{QP} the quasiparticle band gap. The quantity γ is defined as $\gamma = \frac{m_c}{m_c+m_v}$. Since we are considering a model involving a single exciton band, we removed the exciton band index. Moreover we model the electron-phonon matrix elements in Eq. (C2) using a Fröhlich-like interaction for the LO phonon and a Bardeen-Shockley coupling for the LA one,

$$
g_{LO\mathbf{q}} = \frac{i}{|\mathbf{q}|}\left[\frac{4\pi}{V}\frac{\Omega_0}{2}\left(\frac{1}{\epsilon_\infty} - \frac{1}{\epsilon_0}\right)\right]^{1/2}, \tag{C5}
$$

$$
g_{LA\mathbf{q}} = i\left[\frac{1}{2\rho V\varsigma}\right]^{1/2} |\mathbf{q}|^{1/2} D, \tag{C6}
$$

where V is the volume of the primitive cell, ρ is the density of ions, ς the sound velocity, and D is the volume deformation potential. In this way the electron-phonon matrix elements are independent from the electron wave vector $\mathbf{k}$ and the band index $c(v)$.

Insertion of Eq. (C4) and Eqs. (C5) and (C6) into Eq. (C2) leads to the following analytical expression for the square modulus of the exciton-phonon matrix elements:

$$
\left|g^{\mathrm{exc}}_{LO}(\mathbf{q}=0,\bar{\mathbf{q}})\right|^2 = \alpha_{LO}\Omega_0^2 \frac{[I_c(|\bar{\mathbf{q}}|) - I_v(|\bar{\mathbf{q}}|)]^2}{|\mathbf{q}|^2}, \tag{C7}
$$

$$
\left|g^{\mathrm{exc}}_{LA}(\mathbf{q}=0,\bar{\mathbf{q}})\right|^2 = \alpha_{LA}\Omega_D^2 |\bar{\mathbf{q}}| [I_c(|\bar{\mathbf{q}}|) - I_v(|\bar{\mathbf{q}}|)]^2, \tag{C8}
$$

with

$$I_{c(v)}(q) = \frac{1}{\left[1 + \left(\frac{m_{c(v)}}{M}\frac{qa}{2}\right)^2\right]^2}, \tag{C9}$$

and $\alpha_{LO(A)}$ dimensionless constants describing the strength of the coupling with the LO and LA phonons, respectively, and $|\bar{\mathbf{q}}|$ in unit of q_D.

[1] A. L. Fetter and J. D. Walecka, *Quantum Theory of Many-Particle Systems* (McGraw-Hill, New York, 1971).
[2] G. Strinati, Riv. Nuovo Cimento **11**, 1 (1988).
[3] G. Onida, L. Reining, and A. Rubio, Rev. Mod. Phys. **74**, 601 (2002).
[4] K. Hannewald, S. Glutsch, and F. Bechstedt, Phys. Rev. B **62**, 4519 (2000).
[5] G. Stefanucci and R. van Leeuwen, *Nonequilibrium Many Body Theory of Quantum Systems: A Modern Introduction* (Cambridge University Press, Cambridge, 2013).
[6] D. Sangalli and A. Marini, Europhys. Lett. **110**, 47004 (2015).
[7] E. Perfetto, D. Sangalli, A. Marini, and G. Stefanucci, Phys. Rev. B **92**, 205304 (2015).
[8] P. M. M. C. de Melo and A. Marini, Phys. Rev. B **93**, 155102 (2016).
[9] R. Martin, L. Reining, and D. Ceperley, *Interacting Electrons: Theory and Computational Approaches* (Cambridge University Press, Cambridge, UK, 2016).
[10] D. Van Tuan, B. Scharf, I. Žutić, and H. Dery, Phys. Rev. X **7**, 041040 (2017).
[11] Y. Niu, H. Xu, and H. Wei, Phys. Rev. Lett. **128**, 167402 (2022).
[12] D. Tainoff, B. Masenelli, P. Mélinon, A. Belsky, G. Ledoux, D. Amans, C. Dujardin, N. Fedorov, and P. Martin, Phys. Rev. B **81**, 115304 (2010).
[13] I. Akimoto and K. Kan'no, J. Phys. Soc. Jpn. **71**, 630 (2002).
[14] M. Nirmal, C. B. Murray, D. J. Norris, and M. G. Bawendi, Z. Phys. D **26**, 361 (1993).
[15] F. Paleari, H. P. C. Miranda, A. Molina-Sánchez, and L. Wirtz, Phys. Rev. Lett. **122**, 187401 (2019).
[16] E. Cannuccia, B. Monserrat, and C. Attaccalite, Phys. Rev. B **99**, 081109(R) (2019).
[17] H. Y. Chen, D. Sangalli, and M. Bernardi, Phys. Rev. Lett. **125**, 107401 (2020).
[18] G. Strinati, Phys. Rev. Lett. **49**, 1519 (1982).
[19] G. Strinati, Phys. Rev. B **29**, 5718 (1984).
[20] P. Cudazzo and L. Reining, Phys. Rev. Res. **2**, 012032(R) (2020).
[21] P. Cudazzo, Phys. Rev. B **102**, 045136 (2020).
[22] J. S. Zhou, J. J. Kas, L. Sponza, I. Reshetnyak, M. Guzzo, C. Giorgetti, M. Gatti, F. Sottile, J. J. Rehr, and L. Reining, J. Chem. Phys. **143**, 184109 (2015).
[23] J. Lischner, D. Vigil-Fowler, and S. G. Louie, Phys. Rev. Lett. **110**, 146801 (2013).
[24] J. S. Zhou, M. Gatti, J. J. Kas, J. J. Rehr, and L. Reining, Phys. Rev. B **97**, 035137 (2018).
[25] C. Verdi, F. Caruso, and F. Giustino, Nat. Commun. **8**, 15769 (2017).
[26] F. Caruso, C. Verdi, S. Poncé, and F. Giustino, Phys. Rev. B **97**, 165113 (2018).
[27] P. N. Butcher and N. R. Ogg, Proc. Phys. Soc. London **86**, 699 (1965).
[28] R. Enderlein, K. Peuker, and F. Bechstedt, Phys. Status Solidi B **92**, 149 (1979).
[29] L. Hedin and S. Lundqvist, Solid State Phys. **23**, 1 (1970).
[30] F. Giustino, Rev. Mod. Phys. **89**, 015003 (2017).
[31] L. Hedin, J. Phys.: Condens. Matter **11**, R489 (1999).
[32] L. Hedin, Phys. Rev. **139**, A796 (1965).
[33] P. B. Allen and V. Heine, J. Phys. C **9**, 2305 (1976).
[34] P. B. Allen and M. Cardona, Phys. Rev. B **23**, 1495 (1981).
[35] P. M. M. C. de Melo, *Ab initio* approach to photoluminescence based on Green's function theory, Ph.D. thesis, Universidade deCoimbra, 2017.
[36] E. Runge and E. K. U. Gross, Phys. Rev. Lett. **52**, 997 (1984).
[37] R. van Leeuwen, N. E. Dahlen, G. Stefanucci, C. O. Almbladh, and U. von Barth, *Time-Dependent Density Functional Theory*, edited by M. A. Marques, C. A. Ullrich, F. Nogueira, A. Rubio, K. Burke, E. K. Gross, Lecture Notes in Physics, Vol. 706 (Springer, Berlin Heidelberg, 2006).
[38] A. Schindlmayr and R. W. Godby, Phys. Rev. Lett. **80**, 1702 (1998).
[39] I. Tamm, J. Phys. (USSR) **9**, 449 (1945).
[40] S. M. Dancoff, Phys. Rev. **78**, 382 (1950).
[41] F. Paleari and A. Marini, Phys. Rev. B **106**, 125403 (2022).
[42] M. J. Hyrkäs, D. Karlsson, and R. van Leeuwen, J. Phys. A: Math. Theor. **52**, 215303 (2019).
[43] A. Schleife, C. Rödl, F. Fuchs, K. Hannewald, and F. Bechstedt, Phys. Rev. Lett. **107**, 236405 (2011).
[44] M. S. Hybertsen and S. G. Louie, Phys. Rev. B **34**, 5390 (1986).
[45] J. E. Northrup, M. S. Hybertsen, and S. G. Louie, Phys. Rev. B **39**, 8198 (1989).
[46] S. Baroni, S. de Gironcoli, A. Dal Corso, and P. Giannozzi, Rev. Mod. Phys. **73**, 515 (2001).
[47] A. Marini, S. Poncé, and X. Gonze, Phys. Rev. B **91**, 224310 (2015).
[48] A. Marini, Phys. Rev. B **107**, 024305 (2023).
[49] M. Calandra, G. Profeta, and F. Mauri, Phys. Rev. B **82**, 165111 (2010).
[50] G. Marini and M. Calandra, Phys. Rev. B **104**, 144103 (2021).
[51] G. Antonius and S. G. Louie, Phys. Rev. B **105**, 085111 (2022).
[52] F. Aryasetiawan, L. Hedin, and K. Karlsson, Phys. Rev. Lett. **77**, 2268 (1996).
[53] C. Blomberg and B. Bergersen, Can. J. Phys. **50**, 2286 (1972).
[54] F. Aryasetiawan and O. Gunnarsson, Rep. Prog. Phys. **61**, 237 (1998).
[55] M. Vos, A. S. Kheifets, E. Weigold, S. A. Canney, B. Holm, F. Aryasetiawan, and K. Karlsson, J. Phys.: Condens. Matter **11**, 3645 (1999).
[56] A. S. Kheifets, V. A. Sashin, M. Vos, E. Weigold, and F. Aryasetiawan, Phys. Rev. B **68**, 233205 (2003).
[57] M. Guzzo, G. Lani, F. Sottile, P. Romaniello, M. Gatti, J. J. Kas, J. J. Rehr, M. G. Silly, F. Sirotti, and L. Reining, Phys. Rev. Lett. **107**, 166401 (2011).

[58] F. Bechstedt, M. Fiedler, C. Kress, and R. Del Sole, Phys. Rev. B **49**, 7357 (1994).
[59] G. D. Mahan, *Many-Particle Physics*, 2nd ed. (Plenum, New York, 1993).
[60] D. C. Langreth, Phys. Rev. B **1**, 471 (1970).
[61] L. Hedin, Phys. Scr. **21**, 477 (1980).
[62] O. Gunnarsson, V. Meden, and K. Schonhammer, Phys. Rev. B **50**, 10462 (1994).
[63] J. J. Kas, J. J. Rehr, and L. Reining, Phys. Rev. B **90**, 085112 (2014).
[64] J. J. Kas and J. J. Rehr, Phys. Rev. Lett. **119**, 176403 (2017).
[65] P. Král, Phys. Rev. B **56**, 7293 (1997).
[66] H. Fröhlich, Adv. Phys. **3**, 325 (1954).
[67] J. Bardeen and W. Shockley, Phys. Rev. **80**, 72 (1950).
[68] K. Huang and A. Rhys, Proc. R. Soc. London, Ser. A **204**, 406 (1950).
[69] B. Segall and G. D. Mahan, Phys. Rev. **171**, 935 (1968).
[70] J. Bouquiaux, S. Poncé, Y. Jia, A. Miglio, M. Mikami, and X. Gonze, Adv. Opt. Mater. **9**, 2100649 (2021).
[71] S. J. Xu, S.-J. Xiong, and S. L. Shi, J. Chem. Phys. **123**, 221105 (2005).
[72] S. J. Xiong and S. J. Xu, Europhys. Lett. **71**, 459 (2005).
[73] T. Feldtmann, M. Kira, and S. W. Koch, Phys. Status Solidi B **246**, 332 (2009).
[74] S. Shree, M. Semina, C. Robert, B. Han, T. Amand, A. Balocchi, M. Manca, E. Courtade, X. Marie, T. Taniguchi, K. Watanabe, M. M. Glazov, and B. Urbaszek, Phys. Rev. B **98**, 035302 (2018).
[75] C. M. Chow, H. Yu, A. M. Jones, J. R. Schaibley, M. Koehler, D. G. Mandrus, R. Merlin, W. Yao, and X. Xu, npj 2D Mater Appl. **1**, 33 (2017).
[76] M. Combescot and S.-Y. Shiau, *Excitons and Cooper Pairs: Two Composite Bosons in Many-Body Physics* (Oxford Graduate Texts, Oxford, 2015).